Improving the Efficiency of OBBP Allocation Algorithm

Ghazal Rouhafzay

Submitted to the
Institute of Graduate Studies and Research
in partial fulfillment of the requirements for the Degree of

Master of Science
in
Electrical and Electronic Engineering

Eastern Mediterranean University
February 2014
Gazimağusa, North Cyprus

Approval of the Institute of Graduate Studies and Research

Prof. Dr. Elvan Yılmaz
Director

I certify that this thesis satisfies the requirements as a thesis for the degree of Master of Science in Electrical and Electronic Engineering.

Prof. Dr. Aykut Hocanın
Chair, Department of Electrical and Electronic Engineering

We certify that we have read this thesis and that in our opinion, it is fully adequate, in scope and quality, as a thesis of the degree of Master of Science in Electrical and Electronic Engineering.

Assoc. Prof. Dr. Erhan A. İnce
Supervisor

Examining Committee

1. Prof. Dr. Şener Uysal _____

2. Assoc. Prof. Dr. Hasan Demirel _____

3. Assoc. Prof. Dr. Erhan A. İnce _____

ABSTRACT

Mobile WiMAX based on IEEE 802.16e is a broad band wireless access technology which has been widely accepted as the best solution for wireless broad band services. This technology is implemented by Orthogonal Frequency Division Multiple Access (OFDMA) that breaks down the spectrum into narrower bands with smaller number of subcarriers.

In this thesis a comprehensive study of WiMAX system was carried out. We mainly focus on downlink transmission scenario where users assigned by the scheduler should be placed in DL subframe. Different frame packing algorithms are implemented and the work also introduces a new strategy to improve the packing efficiency of the standard Orientation Based Burst Packing (OBBP) algorithm. The aim while packing is to maximize the utilization of the DL subframe space and also at the same time to minimize the wasted slots.

Enhanced One Column Striping with non-increasing Area first mapping (eOCSA) and the OBBP algorithms were first implemented using the MATLAB platform and by introducing a new strategy in the 3rd stage of the OBBP frame packing algorithm a substantial improvement in frame utilization and hence efficiency has been obtained. To start with the efficiency of the modified OBBP (MOBBP) and standard OBBP algorithms were obtained through simulations where a subframe with a capacity of 840 slots (60 subchannels × 28 symbols) was assumed and the instantaneous offered load was varied in the range 0.8 to 3.2. For this set up it was observed that for all offered loads MOBBP had higher efficiencies in comparison

to OBBP. The efficiency gain varied between 1-3 % and was most distinct when the load was around 1 %. In a second experiment, the (eOCSA), OBBP and MOBBP algorithms were compared assuming a subframe with 360 slot capacity (30 subchannels × 12 symbols). For this experiment till the instantaneous load reached 1.5 % the MOBBP would have a 4-5 % improvement in efficiency over OBBP. When the offered load exceeded 1.5 % the gain in efficiency would gradually drop. Comparing eOCSA with OBBP and MOBBP clearly shows that efficiency for eOCSA is consistently better than both over all offered loads. The difference between MOBBP and eOCSA is around 2-2.5 % after the offered load exceeds 2 %. The thesis also provides the mean over allocated slots per frame for the three algorithms compared. By far the eOCSA has the highest over allocated slots among the three compared algorithms. A third experiment was conducted to compare the OBBP and MOBBP under real traffic using the COST-231 Hata Extended channel model. The distance of each user from the base station and speed of user's have been selected from a uniform distribution. We have varied the number of users between 20 and 40. Packing efficiency and number of padded slots in the two algorithms have been compared. For the (30 × 24) DL subframe the results show that MOBBP is again consistently better than the standard OBBP. It was observed that the gain in the frame packing efficiency would change up to 1.2 %.

Keywords: eOCSA; OBBP; MOBBP; OFDMA; DL-PUSC; WiMAX.

ÖZ

IEEE 802.16 standartlarına bağlı bir geniş bant erişim teknolojisi olan WiMAX kablosuz servis sunabilen diğer teknolojiler arasında en iyi çözüm olarak ortaya çıkmaktadır. Bu teknolojinin temelinde dikgen frekans bölüşümlü Çoklu Erişim (OFDMA) yöntemi bulunmaktadır ki bu yöntem frekans bandını katlı ara-taşıyıcılara paylaştırmaktadır.

Bu tezde WiMAX sistemi ve içerdiği alt bloklar kapsamlı bir şekilde çalışılmıştır. Ağırlıkla aşağı bağlantı iletim senaryosu altında çizelgeleyici tarafından atanan kullanıcıların DL altçerçevesine yerleştirilmesi incelenmiştir. Çalışmada farklı çerçeve doldurma algoritmaları kıyaslanmış ve yeni bir strateji doğrultusunda standard OBBP çerçeve dolgulama algorıtmasının altçerçeve kullanım oranı ve dolayısı ile verimlilik yüzdesinin nasıl artırılabileceği gösterilmiştir. Dolgulama esnasında esas hedef DL alt çerçevesini en iyi şekilde kullanma ve ayni zamanda da dilim heba oranını en aza indirmek idi.

İlk olarak MATLAB platforumu üzerinde eOCSA ve OBBP algoritmaları gerçekleştirilmiş ve standard OBBP algoritmasının 3. ayağında yeni bir strateji kullanılarak çerçeve kulanım oranı ve dolayısı ile dolgulama verimliliği önemli oranda iyileştirilmiştir. Başlangıçta, standard OBBP ve geliştirilmiş OBBP (MOBBP) algoritmalarının verimlilikleri 840 dilimli (60 alt kanal × 28 sembol) bir altçerçeve varsayan ve anlık yükü 0.8 ile 3.0 arasında değiştiren benzetim çalışmaları ile elde edilmiştir. Bu deneyde MOBBP nin tüm anlık yüklerde OBBP ye göre daha yüksek verimliliğe sahip olduğu ortaya çıkmıştır. Verimlilik kazancı yüzde 1-3

arasında değişmiş ve en yüksek kazanç yükün 1% oldu durumda görülmüştür. İkinci bir deneyde ise geliştirilmiş eOCSA, OBBP ve MOBBP algoritmaları 360 dilimlik (30 alt kanal × 24 sembol) kapasitesi olan bir alt-çerçeve varsayarak kıyaslanmıştır. Görülmüştür ki anlık yük yüzde 1.5'i aşana kadar MOBBP, standard OBBP ye göre 4-5 % verimlilik kazancı sağlamaktadır. Yükün daha da artırıldığı durumlarda aradaki verimlilik kazanç farkı yavaşça düşmektedir. Bütün anlık yüklerde eOCSA'in verimlilik değerleri hem OBBP hem de MOBBP ye göre daha yüksek bulunmuştur. MOBBP ve eOCSA arasındaki fark anlık yük 2 % bulduktan sonra yaklaşık yüzde 2-2.5 civarındadır. Bildiride ayrıca frame başına her algoritmanın ortalama fazladan özgüleme değerleri de farklı anlık yükler için sunulmuştur. En yüksek fazladan özgüleme yapan algoritmanın eOCSA olduğu görülmüştür.

Bir üçüncü deney de ise COST-231 genişletilmiş Hata kanal modeli gerçekleştirilmiş ve OBBP ve MOBBP algoritmaları gerçek trafik altında kıyaslanmıştır. Kullanıcıların baz istasyonundan uzaklıkları ve her kullanıcının hızı düzgün dağılımlardan çekilmiştir ve sistemdeki kullanıcı sayısı 20 ile 40 arasında değiştirilmiştir.

Her iki algoritmanın altçerçeve doldurma verimliliği ve kaç dilim dolguladığı incelenmiştir. (30 × 24) lük altçerçeveler için MOBBP nin OBBP ye göre devamlı daha iyi sonuç verdiği görülmüştür. Gerçek kanal ve yük altında elde edilen çerçeve dolgulama verimlilik kazancı kadar yüzde 1.2 arasında değişmektedir.

Anahtar Kelimeler: eOCSA; OBBP; MOBBP; OFDMA; DL-PUSC; WiMAX.

Dedicated to

My parents Leili Razeghi and Farhad Rouhafzay

and my sisters Asal and Lael

ACKNOWLEDGMENTS

Firstly, I would like to express my gratitude to my supervisor Assoc. Prof. Dr. Erhan A. İnce for constantly encouraging my research and for being supportive of me whenever I needed his help. His guidance and discussions have been priceless.

I also would like to thank the academic staff at the Electrical and Electronic Engineering department, especially those from whom I had the pleasure of taking courses.

Last but not least I would like to acknowledge my family. I am very grateful to my mother, father and sisters for the sacrifices that they've made on my behalf.

TABLE OF CONTENTS

LIST OF FIGURES

LIST OF TABLES

LIST OF SYMBOLS AND ABBREVIATIONS

BS_{th}	Threshold Burst Size
G_r	Receiver Gain
G_t	Transmitter Gain
P_r	Received Power
P_t	Transmitted Power
$\boldsymbol{\lambda}$	Wavelength
BS	Base Station
BSR	Burst Size Ratio
CP	Cyclic Prefix
COST	Coopération européenne dans le domaine de la recherche Scientifique Technique
DCD	Downlink Channel Descriptor
DFT	Discrete Fourier Transform
DL	Downlink
DL-PermBase	Downlink Permutation Base
DLPF	Down Link Frame Prefix
eOCSA	Enhanced One Column Striping with non-increasing Area first mapping
FCH	Frame Control Header
FFT	Fast Fourier Transform
FUSC	Full Usage Of Sub-Channels
LAN	Local Area Network
LoS	Line of Sight
MAN	Metropolitan Area Network

NLoS	Non Line of Sight
Nsch	Number of Subchannel
Nsymb	Number of Symbols
OBBP	Orientation Based Burst Packing
OF	Orientation Factor
OFDM	Orthogonal Frequency Division Multiplexing
OFDMA	Orthogonal Frequency Division Multiple Access
PL	Pathloss
PUSC	Partial Usage of Subchannels
Qos	Quality of Service
RP_Matrix	Repetition Matrix
RTG	Receive Transition Gap
S-OFDMA	Scalable Orthogonal Frequency Division Multiple Access
TTG	Transmit Transition Gap
UCD	Uplink Channel Descriptor
UL	Uplink
Wi-Fi	Wireless Fidelity
WiMAX	Worldwide Interoperability for Microwave Access
WLAN	Wireless Local Area Network
PAN	Personal Area Network
WPAN	Wireless Personal Area Network

Chapter 1

INTRODUCTION

Wireless communications and its related products have found their ways into our everyday lives. There are many available standards describing communication parameters for devices such as Bluetooth and 802.11 but they are not capable to provide sufficient data rate, for high-speed moving users. To deal with this problem an IEEE workgroup has proposed 802.16 standards which not only supports fixed Line of sight (LoS) communication (10-66 GHz) but also describes Non-LoS wireless communication (2-11 GHz) for mobiles moving at speeds as high as 125 km/h . (802.16e).

Five wireless technologies have managed to make an impact among many that have been proposed. These successful technologies include wireless global area networks (WGANs), wireless personal area networks (WPANs), wireless local area networks (WLANs), wireless broadband–personal area networks (WB-PANs) and wireless wide area networks (WWANs) have been depicted in Figure 1.1.

Wireless Personal Area Networks (WPANs) and Personal Area Networks (PANs) are data networks which communicate among data devices around one person (in a 10 m range) and for different QoS have low data rates. Examples for WPANs include IEEE 802.15, HIPERPAN and Bluetooth. LANs and WLANs would communicate among data devices in short ranges such as 100-200 meters.

Metropolitan Area Networks (MANs) on the other hand can cover more than several kilometers and the most widely studied technologies include wireless mesh and WiMAX.

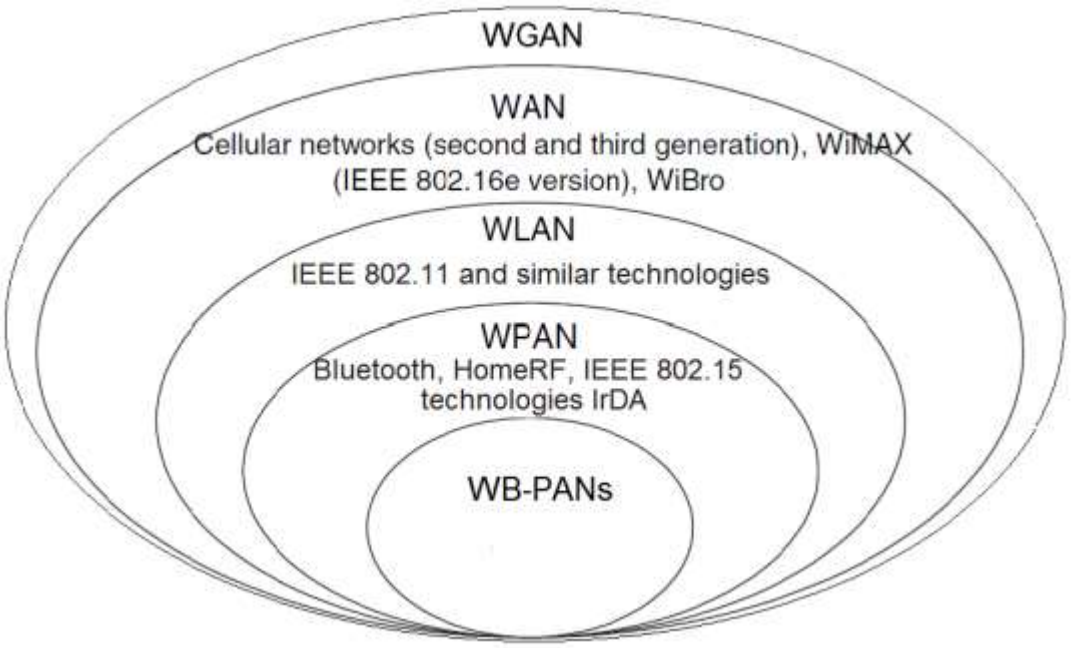

Figure 1.1: Network Types [1]

Different Types of applications can be supported by WiMAX; voice, video, data and multimedia are some examples. Each application requires different data rate, delay, packet loss and traffic pattern. A large number of users are also supported by Mobile WiMAX, and each user has a particular QoS requirement.

WiMAX is well implemented by OFDMA. In OFDMA instead of using a single wide-band carrier, multiple subcarriers which are narrow-band and parallel are used to transmit information. Based on the bandwidth subcarriers can be grouped into different number of subchannels. The method of grouping the subcarriers to form a subchannel is known as subchannelization. OFDMA can also combat ISI by

applying a guard interval between OFDM symbols. These features enable OFDMA to improve the system capacity.

One slot, consisting 48 data sub-carriers is the minimum frequency-time resource unit of subchannelization. Based on the subchannelization scheme a slot can be defined as one subchannel over 1, 2, or 3 OFDM symbols. Subcarrier permutation is possible either using distributed or contiguous (adjacent) permutation. The distributed permutation modes include DL-FUSC, DL-PUSC and UL-PUSC. The contiguous permutation modes are used for DL-AMC and UL-AMC. A WiMAX frame using time division duplexing mode has been shown in Figure 1.2. Generally, frame sizes can vary from 2 ms to 20 ms, however WiMAX devices available on the market have been designed for the 5 ms frame.

As depicted by Figure 1.2 a WiMAX frame consists of a downlink and an uplink subframe separated by the transmit transition gap (TTG). Different downlink-to-uplink subframe ratios can be adopted. Most often used ratios include 3:1 and 1:1.

In a DL subframe several slots assigned to a Mobile Station (MS) are called a burst. In fact the bursts carry user's data. Based on QoS provisioning, scheduler determines bursts sizes. The mobile WiMAX standard states that the shape of the bursts should be rectangular. This requirement makes burst packing problem a more challenging task.

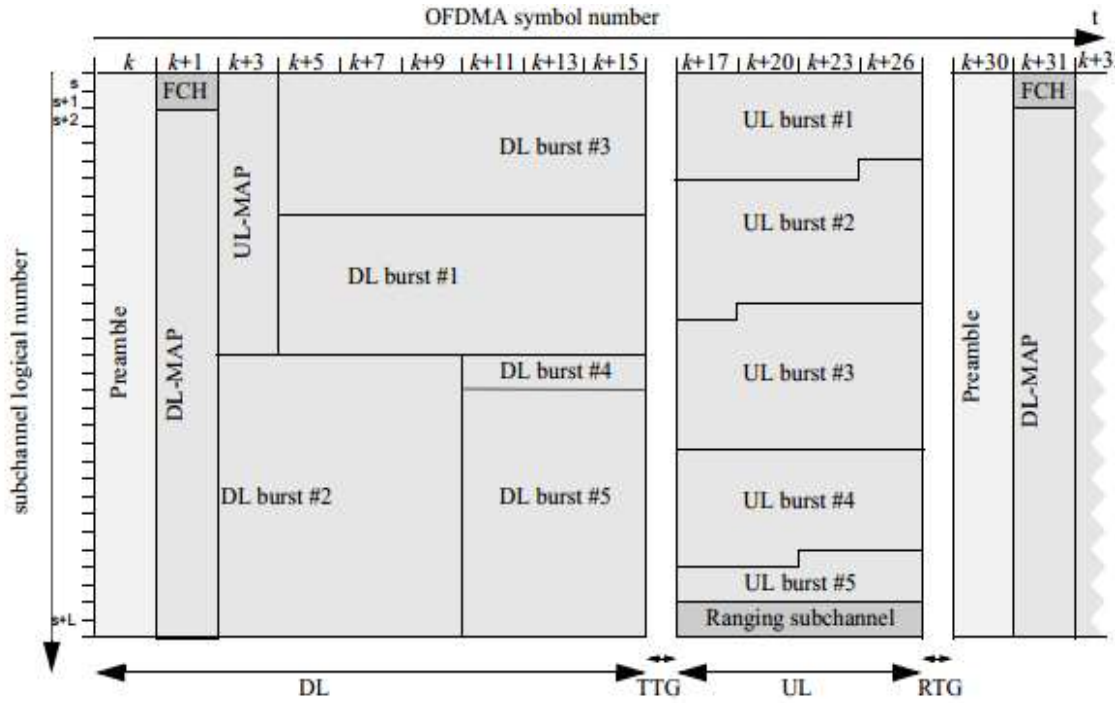

Figure 1.2: WiMAX Frame Structure [2]

Several frame packing algorithms have been presented which trying to minimize the number of unused slots and over allocations. OCSA, eOCSA, OBBP, are some examples. In this work we have tried to address the DL burst mapping problem building upon orientation-based burst packing algorithm described in [3]. In particular, we try to improve the frame packing efficiency of the algorithm by introducing a new packing strategy in the third stage of the OBBP algorithm. The modified version of the OBBP algorithm is referred to as the MOBBP. Comparative simulation results for packing efficiency of OBBP, MOBBP and eOCSA are provided for two different size DL subframes and under various instantaneous offered loads. Mean over allocated slots per frame under different instantaneous offered loads is also provided for the eOCSA, OBBP and MOBBP algorithms. Figure 1.3 illustrates an OFDMA subframe filled by rectangular bursts.

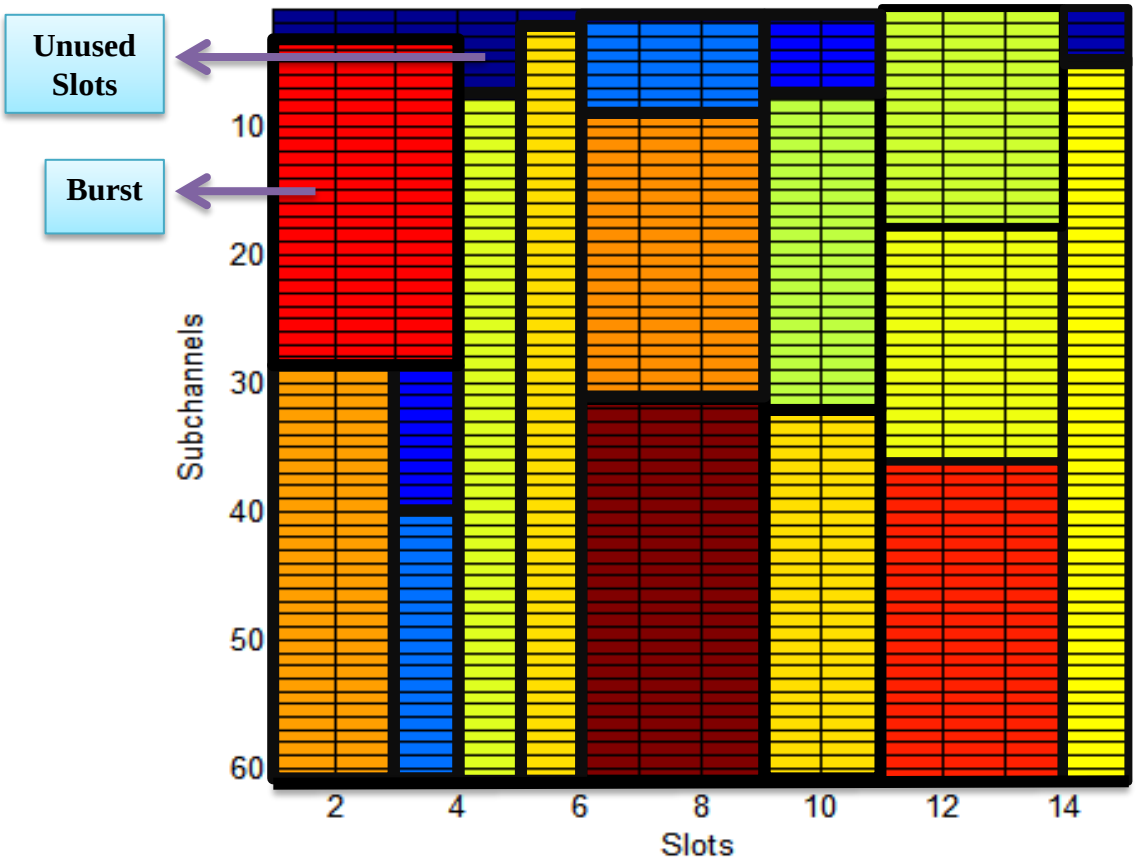

Figure 1.3: Rectangular Bursts and unused slots in a subframe

1.1 WiMAX Background

In 1990, internet service providers suggested to use fixed broad band wireless networks to deliver Internet service to their users. They targeted to combine particular features of hardwired networks and wireless networks to create a low cost reliable and flexible network with high speed and high capacity. Local Multipoint Distribution Services (LMDS) and Multi-channel Multipoint Distribution Services (MMDS) were proposed for use in fixed wireless broadband services. In particular, the MMDS was used to provide wireless broadcast for video services. Consequently, in 1999 the standard for local multipoint distributed services was created by IEEE 802.16 group. The standard adopted a point-to-point connection and had LOS transmissions in a frequency range of 10-66 GHz.

WiMAX Forum was established in 2001 to promote the adoption of WiMAX products and services. Later in 2003 the IEEE802.16a was formulated to transmitted data from omni-directional antennas over NLOS radio channels.

Fixed WiMAX (802.16-2004) has been an efficient substitute for cable and DSL technologies. In 2005, IEEE 802.16e amendment has brought the ability to support mobility. IEEE 802.16e amendment also proposed SOFDMA which can support scalable channel bandwidths from 1.25 to 20 MHz. Over a 10 MHz channel, mobile WiMAX based on IEEE 802.16e standard can provide data rates up to 63 Mbps and 28 Mbps per sector for DL and UL respectively [3].

The certification profiles for mobile and fixed WiMAX are shown in Table 1.1. The duplexing mode, channel bandwidth and frequency band are specified in the profiles.

1.2 Thesis Description

In this thesis we have introduced a new packing strategy in the third stage of the well-known OBBP frame packing algorithm that helps attain better utilization of the available free space in the DL subframe and hence leads to an increased frame packing efficiency. Three algorithms, namely; the standard OBBP algorithm, the modified OBBP (MOBBP) algorithm and eOCSA algorithm have been implemented using the MATLAB platform. All three algorithms have been simulated for different frame sizes and instantaneous offered loads and efficiency and mean over allocation values have been obtained for (i) randomly generated bursts and (ii) for realistic channel models like the COST-231 Extended Hata channel.

Table 1.1: Versions of WiMAX [4]

	802.16	**802.16-2004**	**802.16-2005**
Application	None	256 - OFDM as Fixed WiMAX	SOFDMA as Mobile WiMAX
Bandwidths	20MHz, 25MHz, 28MHz	1.75MHz, 3.5MHz, 7MHz, 14MHz, 1.25MHz, 5MHz, 10MHz, 15MHz, 8.75MHz	1.75MHz, 3.5MHz, 7MHz, 14MHz, 1.25MHz, 5MHz, 10MHz, 15MHz, 8.75MHz
Constellation Mapping	QPSK, 16 QAM 64 QAM	QPSK 16 QAM 64 QAM	QPSK 16 QAM 64 QAM
Architecture	Point-to-multipoint	Point-to-multipoint	Point-to-multipoint
Reserved Frequencies	10–66 GHz	2–11 GHz	Mobile applications: 2–6GHz Fixed applications: 2–11GHz
Data rate	32–134.4Mbps	1–75Mbps	1–75Mbps
Mode of Multiplexing	TDMA	OFDMA	OFDMA
Mode of Duplexing	FDD /TDD	FDD /TDD	FDD / TDD

1.3 Thesis Contributions

We have showed that under all instantaneous offered loads the efficiency of MOBBP would be better than that of standard OBBP's. This would hold for both randomly generated bursts and for uniform deployment of mobile subscribers in a macrocell assuming a realistic channel such as the COST-231Extended Hata.

1.4 Thesis Overview

Following the introduction section provided in Chapter 1, Chapter 2 discusses OFDM and OFDMA systems, their features, advantages and application in WiMAX. Chapter 3 is assigned to details of the WiMAX PHY layer and different subchannelization schemes. Chapter 4 contains discussion about Channel model and channel parameters for WiMAX systems. In Chapter 5 we present an effective algorithm for burst packing. Chapter 6 provides the simulation results and discussion. Chapter 7 makes conclusions and gives directions for future work.

Chapter 2

OFDM VS OFDMA

OFDM is a digital modulation technique which uses multiple subcarriers to transmit a single signal. That means a very fast signal is separated into several slow ones. The subchannels transmit data without facing the same amount of multipath distortion for a single carrier transmission, so mobile access is also optimized. Figure 2.1 (a) depicts multi-carrier concept of OFDM transmission scheme. A multi-user system can be generated by using OFDM together with CDMA, TDMA and FDMA.

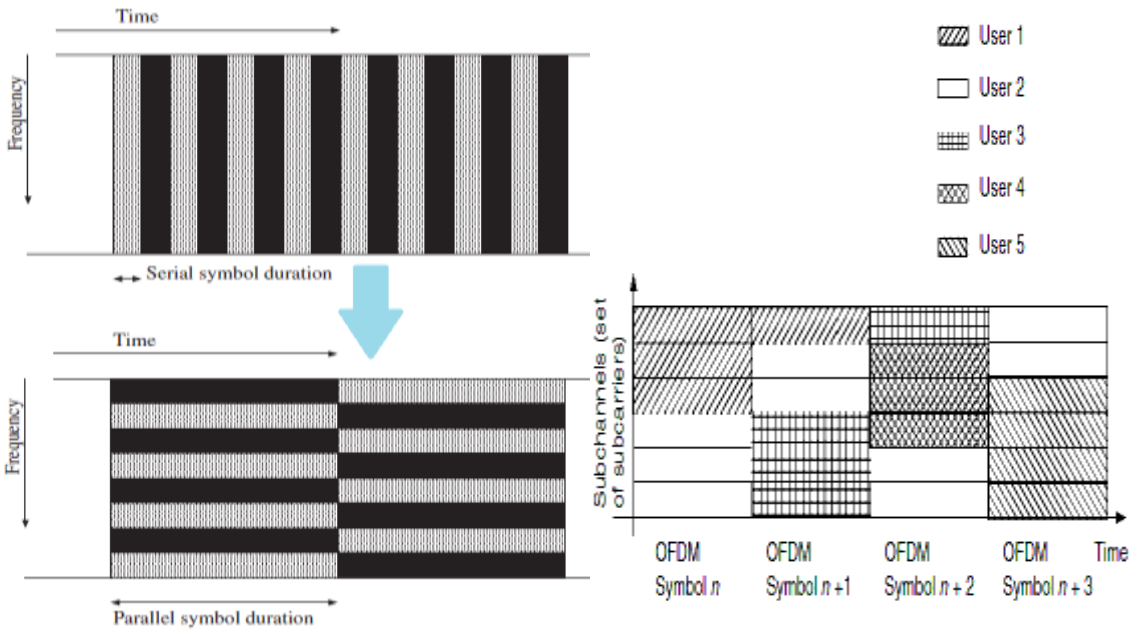

(a) (b)

Figure 2.1: OFDM vs OFDMA (a) Multi Carrier Concept of OFDM [5] (b) Multi Users Concept of OFDMA [1]

The advantage of OFDMA to OFDM is the capability of OFDMA to allocate a subset of subcarriers to individual users. OFDM symbol subcarriers are orthogonally divided among users. The multi-user concept of OFDMA systems is illustrated in Figure 2.1 (b). Table 2.1 depicts the differences between single-carrier and multi-carrier transmission schemes.

Table 2.1: OFDM Based Transmission Schemes [6]

	Single Carrier (SC)	**Multi Carrier(MC)**	**Multi Carrier(MC)**
		OFDM/DMT	**FMT**
Subcarrier spacing	____	$1/T_s$	$1/T_s$
Pulse shape	raised-cosine filter	Rectangular	raised-cosine filter
Guard interval	Not required	Required	Not required
Guard band	Not required	Required	Not required

2.1 Orthogonality

Figure 2-2 shows the spectrums of the subcarriers that are overlapped. This overlapping brings a saving in the bandwidth. Even though the spectrums overlap the information transmitted over the carriers can still be separated because of their orthogonality. OFDM systems rely on the IFFT for signal modulations on the transmitter side. Using IFFT makes all other signals to be zero at the frequency where we evaluate the received signal. To preserve this orthogonality the receiver and the transmitter need to be synchronized .We use FFT in receiver to demodulate the signal.

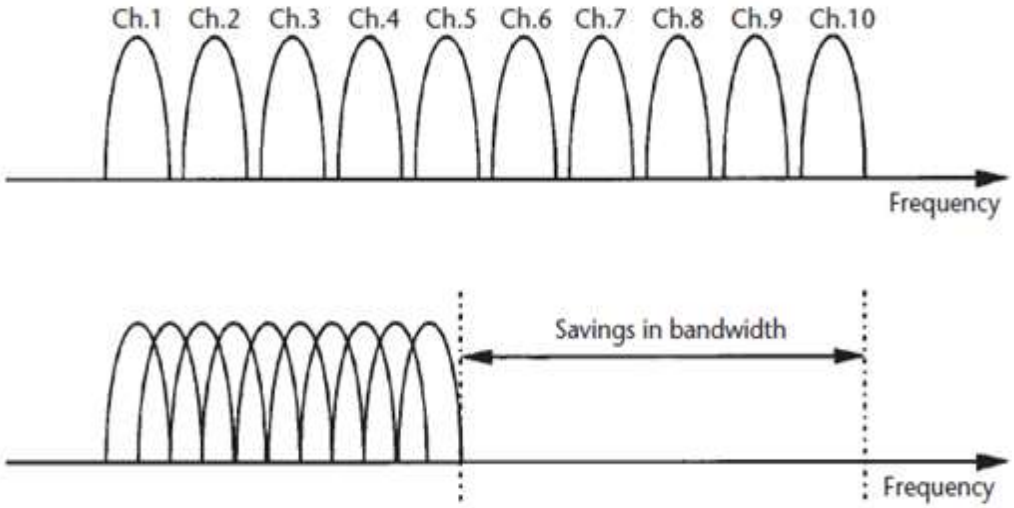

Figure 2.2: Overlapped spectrums of subcarriers in OFDM [7]

2.2 Fourier Transform

Since in OFDM the subcarrier frequencies are selected orthogonal to each other this enables efficient modulator and demodulator implementations using FFT and IFFT as explained in the sections that follow.

2.2.1 DFT and IDFT

The discrete Fourier transform can be employed to transpose a discrete signal into its discrete frequency domain representation. It is important to note that DFT is different with DTFT as DFT remains also discrete in frequency domain. The equation for DFT and its inverse transform IDFT are as follows:

$$X[k] = \sum_{n=0}^{N} x[n] e^{-jkw_0 n} \quad , \quad k = 0,1,\cdots,(N-1) \tag{2.1}$$

$$x[n] = \frac{1}{N} \sum_{n=0}^{N} X[k] e^{jkw_0 n} \quad , \quad n = 0,1,\cdots,(N-1) \tag{2.2}$$

$X[k]$ and $x[n]$ represent the time and frequency domain samples respectively, N is the length of the input sequence and $\omega_0 = \frac{2\pi}{N}$.

2.2.2 FFT and IFFT

FFT is not a new transform; it's just an efficient computational tool to calculate DFT. For FFT/IFFT implementation N should be a power of 2. In FFT algorithm a sample signal is multiplied successively by complex exponentials in frequency range. Sum of each product will be the coefficient of that frequency. These coefficients describe the presence of each frequency in the composite signal. In an OFDMA system number of sub-carriers is equal to the FFT size, for example in a system with 256 sub-carriers, the FFT size will also be 256.

2.3 Effects of Inter Symbol Interference (ISI) and Inter Carrier Interference (ICI)

When a transmitted signal reaches the receiver trough several paths, frequency selective multipath propagation may cause Inter Symbol Interference. In Figure 2.3, L data symbols are grouped into a block representing an OFDM symbol. The symbol duration is T seconds. To prevent interference between OFDM symbols passing a wireless channel, a guard time is defined between them. When the RMS delay spread of the channel (τ) is smaller than the selected guard time, the degrading effect of the multipath channel will be avoided. While introducing the guard interval either zero padding (ZP) or cyclic extension of the OFDM symbol can be used.

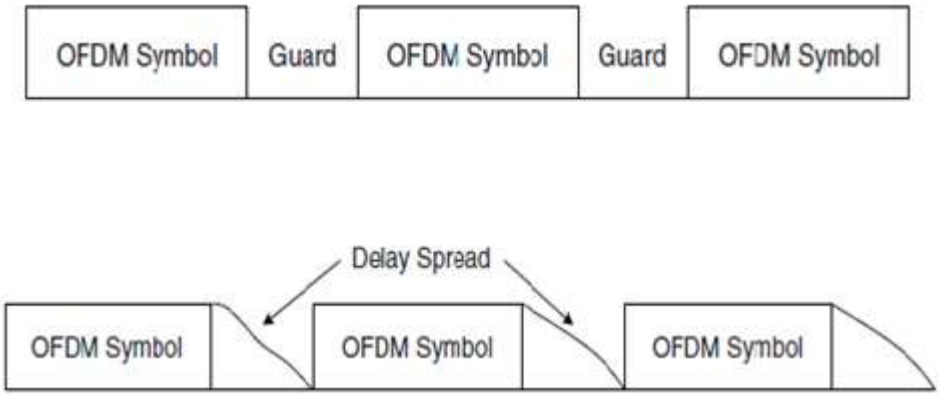

Figure 2.3: Guard time between symbols [4]

Then by applying a circular convolution between the DFT of the input and the channel frequency response, ISI and ICI can be greatly mitigated. This circular convolution can be implemented by concatenating a cyclic prefix to the original data to transmit. Consider the following vector as an OFDM symbol in time domain.

$$X = [x_1 \ x_2 \ x_3 \ \dots \ x_L] \tag{2.3}$$

Applying a cyclic prefix of length *v* we will have

$$X_{cp} = [x_{L-v} \ x_{L-v+1} \ \dots \ x_{L-1} \ x_0 \ x_1 \ x_2 \ \dots \ x_{L-1}] \tag{2.4}$$

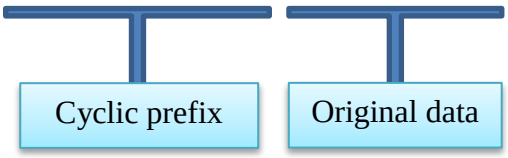

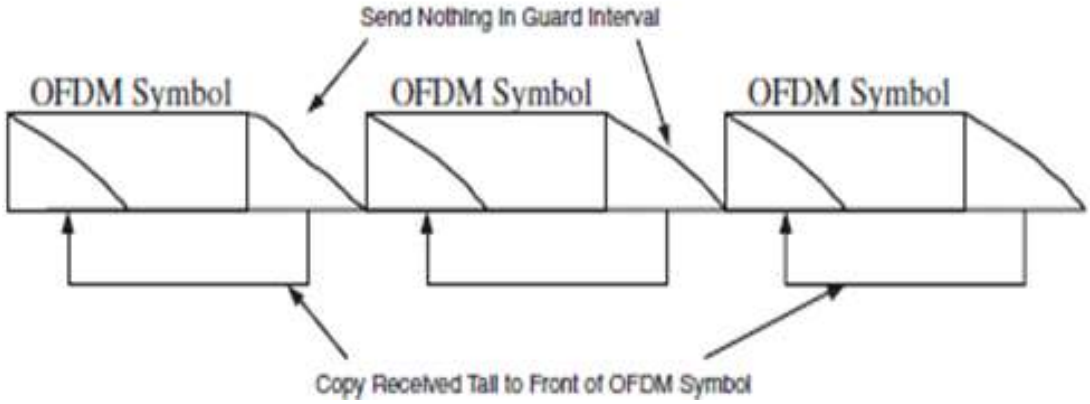

Figure 2.4: Concatenation of cyclic prefix to OFDM symbol [4].

Beside ISI another type of interference introduced by the Doppler shift is Inter Carrier Interference (ICI). It is known that OFDM divides the spectrum into narrowband orthogonal subcarriers. To preserve the orthogonality the subcarriers are required to be spaced exactly in the reciprocal of the symbol period. ICI will start to occur when we have some loss of orthogonality. Both OFDM and OFDMA systems are known to be very sensitive to ICI because of narrow separation between subcarriers.

When a cyclic prefix of length *v* is employed, *v* extra symbols need to be transmitted and the required bandwidth will increase from B to $\left(L + {}^{v}/_{L}\right)B$. Similarly the transmitted power will change from $10 \log_{10} B$ dB to $10 \log_{10}(L + {}^{v}/_{L})B$ dB. Figure 2.5 depicts the OFDM symbol with CP in both time and frequency perspective

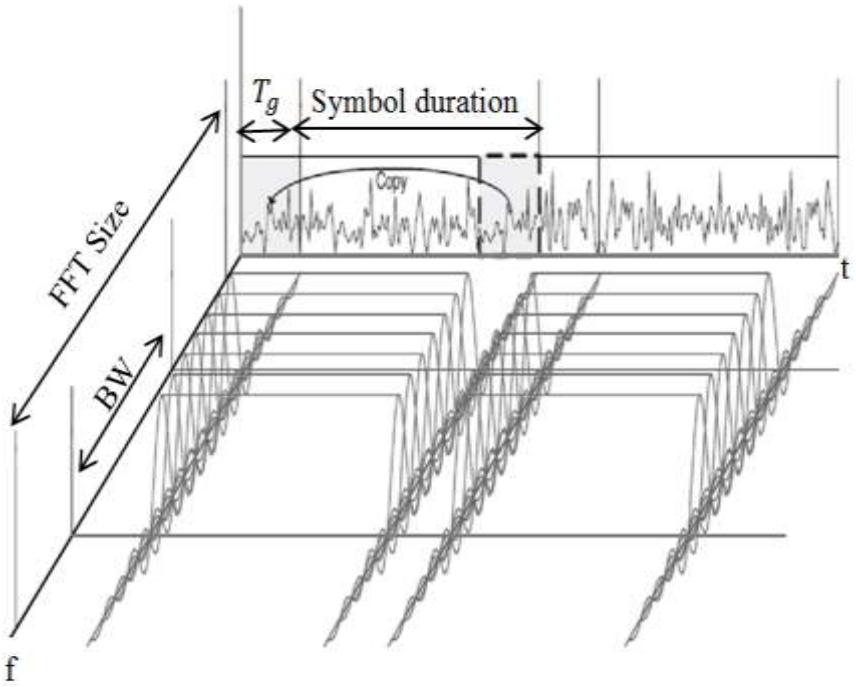

Figure 2.5: Time and Frequency domain representations of OFDM symbol with cyclic prefix [6].

2.4 OFDM Signaling

The *k*-th OFDM symbol for continuous-time signals can be written as

$$S_{RF,k}(t-kT)=Re\left\{w(t-k)\sum_{i-\frac{N}{2}}^{\frac{N}{2}-1}x_{i,k}e^{j2\pi\left(f_c+\frac{i}{T_{FFT}}\right)(t-kT)}\right.$$
$$When\ (kT-T_{win}-T_{guard})\le t\le(kT+T_{FFT}+T_{win}\ ) \quad (2.5)$$

Otherwise $S_{RF,k}(t-kT)$ is equal to zero.

Where, T is the symbol duration, T_{FFT} is the FFT time, T_{guard} is the duration of the guard interval, F = 1/ T_{FFT} is the frequency spacing between subcarriers, f_c is the carrier frequency, N is the number of subcarriers and $x_{i,k}$ denotes the signal constellation points.

The transmitter pulse shape $w(t)$ used in (2.5) is defined as:

$$w(t) = \begin{cases} \frac{1}{2}\left[1 - \frac{\cos\pi(t+T_{win}+T_{guard})}{T_{win}}\right] & -T_{win} - T_{guard} \le t < -T_{guard} \\ 1 & -T_{guard} \le t \le T_{FFT} \\ \frac{1}{2}\left[1 - \frac{\cos\pi(t-T_{FFT})}{T_{win}}\right] & T_{FFT} < t \le T_{FFT} + T_{win} \end{cases} \quad (2.6)$$

A sequence of transmitted OFDM symbols can be expressed as:

$$S_{RF}(t) = \sum_{k=-\infty}^{\infty} S_{RF,k}\,(t - kT) \quad (2.5)$$

Figure 2.6 depicts the block diagram of an OFDM transmitter and receiver. Initially OFDM was designed to transmit a single signal over multiple subcarriers. OFDMA which is a multiple access version of OFDM allocates a subset of subcarriers to individual users. In each OFDM symbol subcarriers are orthogonally divided among all users which make it the multi-user version of OFDM. Scalable OFDMA (S-OFDMA) is an improved version of OFDMA. Small FFT sizes are more suitable for channels with low bandwidths, while larger FFT sizes are used for wider channels. In SOFDMA by keeping the subcarrier frequency spacing constant at 10.94 KHz (symbol duration at $91.4\ \mu s$) one can scale the FFT size to the channel bandwidth which will decrease the complexity of the system for smaller channels and improve the performance. The SOFDMA parameters are provided in Table 2.2.

Table 2.2: SOFDMA parameters [1]

Parameter	Possible Values			
FFT length	128	512	1024	2048
Sample rate	1.4	5.6	11.2	22.4
Channel Bandwidth (MHz)	1.25	5	10	20
Number of Sub-Channels	2	8	16	32

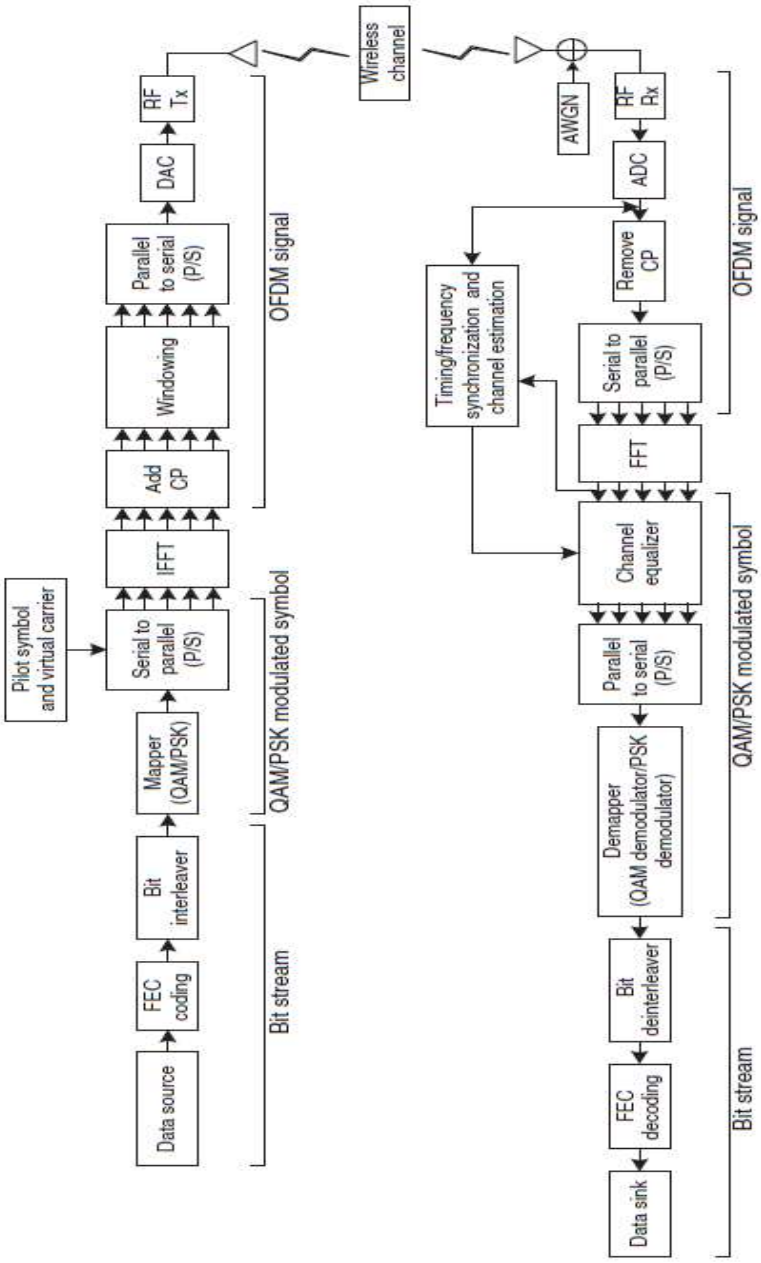

Figure 2.6: OFDM transceiver [6]

Chapter 3

WIMAX PHYSICAL LAYER

WiMAX Physical layer is based on the IEEE 802.16 and IEEE 802.16e standards. For operation in different frequency bands four different physical layers have been defined. Also, for use in license exempt bands High-speed Unlicensed Metropolitan Area Network (HUMAN) have been specified. The various physical layers and the frequency bands they operate in have been listed below:

- Wireless MAN SC (single-carrier, 11-66 GHz, LoS communication).
- Wireless MAN SCa (single-carrier, 2-11GHz, point-to-multipoint).
- WirelessMAN OFDM or fixed WiMAX (256-point OFDM, 2-11 GHz, NLOS communication)
- WirelessMAN OFDMA, (2,048-point OFDMA, 2-11 GHz band, NLoS communication)

A WiMAX transmitter is composed of a randomizer, forward error correction (FEC) coder, an interleaver and a constellation mapper. The block diagram in Figure 3.1 shows the main functional blocks that make up the physical layer of WiMAX transmitter. Channel encoder, the interleaver, and constellation mapper are related to FEC. The space/time encoder and subcarrier allocation and pilot insertion blocks are responsible for constructing the OFDM symbol. The remaining blocks transform the

OFDM signal into an analogue form that can be transmitted from the multiple antennas.

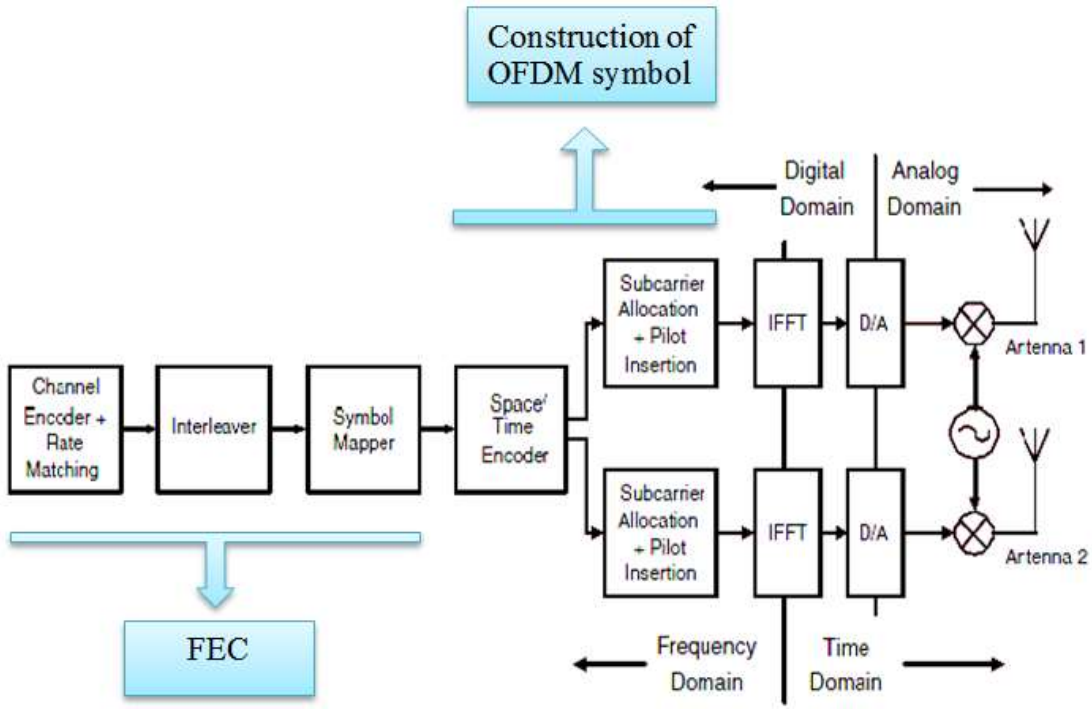

Figure 3.1: Functional stages of WiMAX PHY [4]

As we have already discussed, generating an OFDM symbol requires mapping the modulated symbols into subchannels. A subchannel is composed of a group of subcarriers. There are four types of subcarriers in WiMAX. Mainly;

- The DC subcarrier
- Data subcarriers
- Pilot subcarriers (channel estimation and synchronization)
- Null subcarriers for the guard bands.

The WiMAX standards come with two duplexing modes, namely; time division duplexing (TDD) and frequency division duplexing (FDD). In FDD uplink and downlink channels are on different frequencies.

3.1 Subcarrier Permutation Modes

There are several effective parameters to determine number of subchannels assigned to transmit a data block. Some of these parameters are the data block size, the selected constellation mapping, and the coding rate. The subcarriers that constitute subchannels may come from adjacent frequencies or they may be from different parts of the spectrum. In distributed permutation we will have a wide frequency range, but in adjacent subcarrier distribution the system can exploit multiuser diversity.

3.1.1 DL Full Usage of Subchannels (DL-FUSC)

In DL-FUSC, the whole data subcarriers are in use to constitute different subchannels. 48 data subcarriers from the entire spectrum are in use to form a subchannel. There are totally $48 \times 32 = 1536$ data subcarriers (including the guard and DC subcarriers) where the subchannel indices are expressed by a Reed-Solomon series. In FUSC first all the pilot subcarriers are allocated, and then the rests of the subcarriers will be used to define the data subchannels. Pilot subcarriers belong to four different sets. Two sets among four are constant and two are variable. Pilot subcarriers of the variable sets have a unique index for each OFDM symbol, however the pilot subcarriers of the constant sets have invariant index. The variable set of pilots inserted in the symbol of each segment obeys the following equation:

$$\text{PilotsLocation} = \text{VariableSet}\ x\ + 6 \cdot (\text{FUSC SymbolNumber} \ \%\ 2) \qquad (3.5)$$

Where, Symbol Number represents the FUSC symbols used in current zone.

Figure 3.2 below depicts the general processing in FUSC subcarrier permutation mode and Table 3.1 shows the various parameters of FUSC permutation scheme for different FFT sizes.

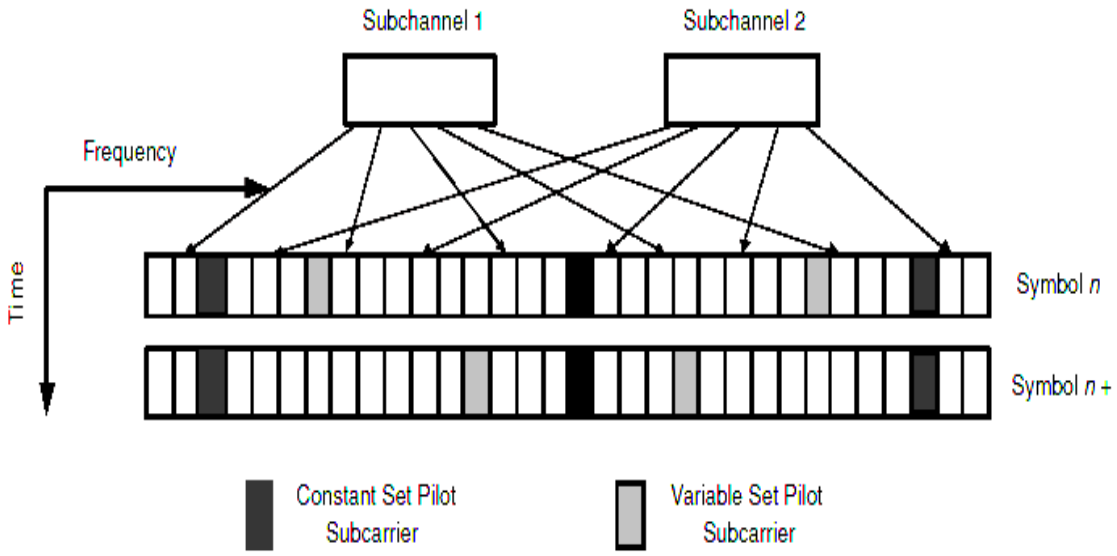

Figure 3.2: FUSC subcarrier permutation scheme [4]

Table 3.1: Parameters of FUSC permutation scheme for different FFT sizes [4]

	128	**512**	**1024**	**2048**
Number of subchannels	2	8	16	32
Subcarriers per subchannel	48	48	48	48
Data subcarriers used	96	384	768	1536
Pilot subcarrier in constant Set	1	6	11	24
Pilot subcarriers in variable Set	9	36	71	142
Left-guard subcarriers	11	43	87	173
Right-guard subcarriers	10	42	86	172

The allocation of the data subchannels is done by dividing the subcarriers into groups of adjacent subcarriers. Each subchannel contains one subcarrier from each of these groups. The exact partitioning into subchannels is as follows:

$$\text{Subcarrier } (k,\ s) = N_{subchannels} \cdot n_k + \{p_s[n_k mod\ N_{subchannels}] + DL\_PermBase\} \bmod N_{subchannels} \quad (3.5)$$

Where, subcarrier (n,s) represents the subcarrier index of n-th subcarrier in the s-th subchannel, $n_k = (k + 13 \cdot s) mod N_{subcarriers}$ where $N_{subcarriers}$ is 24 for DL-PUSC, $N_{subchannels}$ are the number of subchannels based on the bandwidth , $P_s(j)$ is the sequence obtained by cyclically rotating the basic permutation sequence to the left *s* times and DL_PermBase is an integer in the range 0 - 31.

3.1.2 Downlink Partial Usage of Subcarriers (DL-PUSC)

In DL-PUSC subcarriers are divided into six clusters. As illustrated in Figure 3.3 each cluster is made up of 14 adjacent subcarriers by two OFDM symbols. These 28 subcarriers include 4 pilot subcarriers and 24 data ones. Then a pseudorandom numbering scheme is used to re-number the clusters and after that they will be divided into six groups.

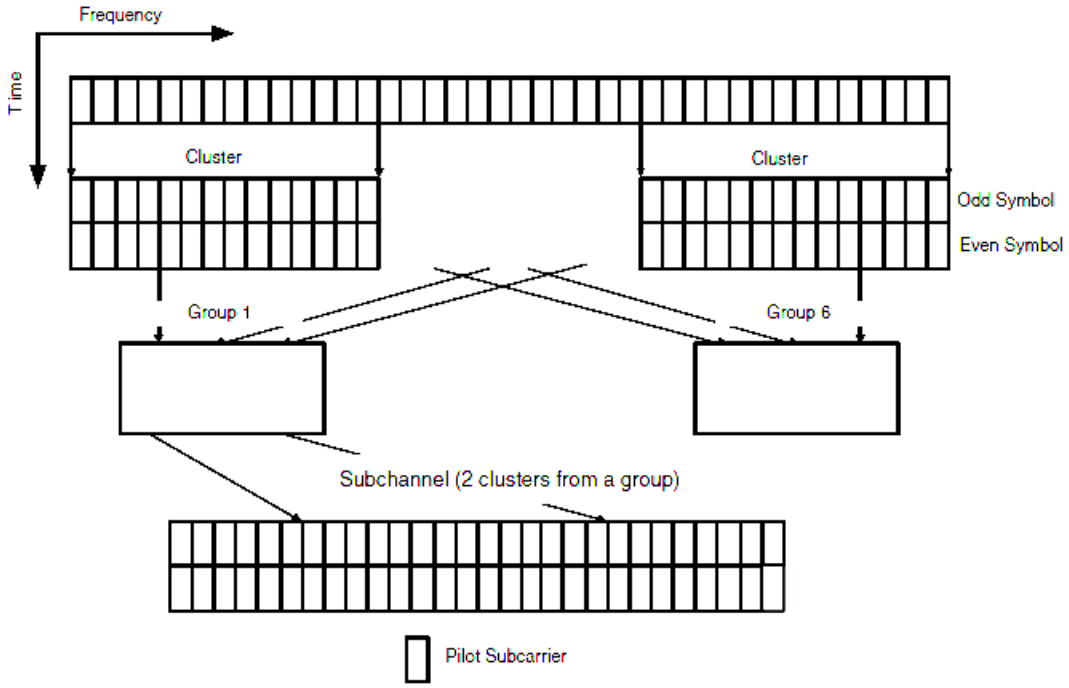

Figure 3.3: DL PUSC subcarrier permutation scheme [4]

Parameters of DL PUSC Subcarrier Permutation are represented in Table 3.2.

Table 3.2: Parameters of DL PUSC Subcarrier Permutation [4]

	128	**512**	**1024**	**2048**
Number of subchannels	3	15	30	60
Subcarriers per cluster	14	14	14	14
Data subcarriers used	72	360	720	1440
Pilot subcarriers	12	60	120	240
Left-guard subcarriers	22	46	92	184
Right-guard subcarriers	21	45	91	183

Allocating subcarriers into subchannels in DL-PUSC is performed as detailed below: Grouping the subcarriers into different physical clusters ($N_{clusters}$), each cluster will be made up of 14 adjacent subcarriers (starting from carrier 0). $N_{clusters}$ changes with FFT sizes.

- Physical cluster to logical cluster renumbering is done using

LogicalCluster=

$$\begin{cases} RenumberingSequence\ (PhysicalCluster) & First\ DL\ zone, or\ Use\ All\ SC\ indicator\ =\ 0 \\ RenumberingSequence\left((PhysicalCluster) + 13 \cdot \mathrm{DL}_{\mathrm{premBase}}\right) mod\ Nclusters & Otherwise \end{cases} \quad (3.6)$$

Table 3.3 represents renumbering sequence for different FFT sizes

Table 3.3: Renumbering sequences for different FFT sizes [2]

FFT Size	2048	1024	512	128
Renumbering sequence	6, 108, 37, 81, 31, 100, 42, 116, 32, 107, 30, 93, 54, 78, 10, 75, 50, 111, 58, 106, 23, 105, 16, 117, 39, 95, 7,115, 25, 119, 53, 71,22, 98, 28, 79, 17, 63, 27, 72, 29,86, 5, 101, 49, 104, 9, 68, 1, 73, 36, 74, 43, 62, 20, 84,52, 64, 34, 60, 66, 48, 97, 21, 91, 40, 102, 56, 92, 47, 90, 33, 114, 18, 70, 15, 110, 51, 118, 46, 83, 45, 76, 57, 99, 35, 67, 55, 85, 59, 113, 11, 82, 38, 88, 19, 77, 3, 87, 12, 89, 26, 65, 41, 109, 44, 69, 8, 61,13, 96, 14, 103, 2, 80, 24, 112, 4, 94, 0	6, 48, 37, 21, 31, 40, 42, 56, 32, 47, 30, 33, 54, 18, 10, 15, 50, 51, 58, 46, 23, 45, 16, 57, 39, 35, 7, 55, 25, 59, 53, 11, 22, 38, 28, 19, 17, 3, 27, 12, 29, 26, 5, 41, 49, 44, 9, 8, 1, 13, 36, 14, 43, 2, 20, 24, 52, 4, 34, 0	12, 13, 26, 9, 5, 15, 21, 6, 28, 4, 2, 7, 10, 18, 29, 17, 16, 3, 20, 24, 14, 8, 23, 1, 25, 27, 22, 19, 11, 0	2, 3, 1, 5, 0, 4

- Allocating logical clusters to groups. The allocation algorithm varies for different FFT sizes.
- Allocating subcarriers to subchannel in each group which will be implemented for all OFDMA symbols independently. First the pilot carriers are allocated in each cluster, and then data carriers will be taken within the symbol using (3.5) which was also used in the case of DL-FUSC. The parameters vary with FFT sizes.

Table 3.4 demonstrates the parameters used in (3.6) for different FFT sizes.

Table 3.4: Parameters used in equation (3.6) for different FFT sizes

FFT size	**2048**	**1024**	**512**	**128**
$\mathbf{N_{Subchannels}}$	60	30	15	3
$\mathbf{N_{Subcarriers}}$	24	24	24	24
DL permBase	6,9,4,8,10,11,5,2,7,3,1,0 7,4,0,2,1,5,3,6	3,2,0,4,5,1 3,0,2,1	4,2,3,1,0	___

3.1.3 Uplink Partial Usage of Subcarriers

As illustrated in Figure 3.4 in UL-PUSC, we firstly divide the subcarriers into multiple tiles. Each tile contains four subcarriers by three OFDM symbols $4 \times 3 = 12$. These 12 subcarriers in a tile include eight data subcarriers and four pilot subcarriers. We re-number the tiles by a pseudorandom numbering scheme. Then the tiles will be divided into six groups and six tiles from a particular group will form a subchannel.

3.2 WiMAX Frame Structure

In TDD mode WiMAX PHY frames are divided to downlink and uplink subframes. TTG gap separates downlink subframe from uplink and the uplink subframe is separated from the subsequent downlink by RTG gap. Figure 3.5 shows the formation of a WiMAX PHY frame.

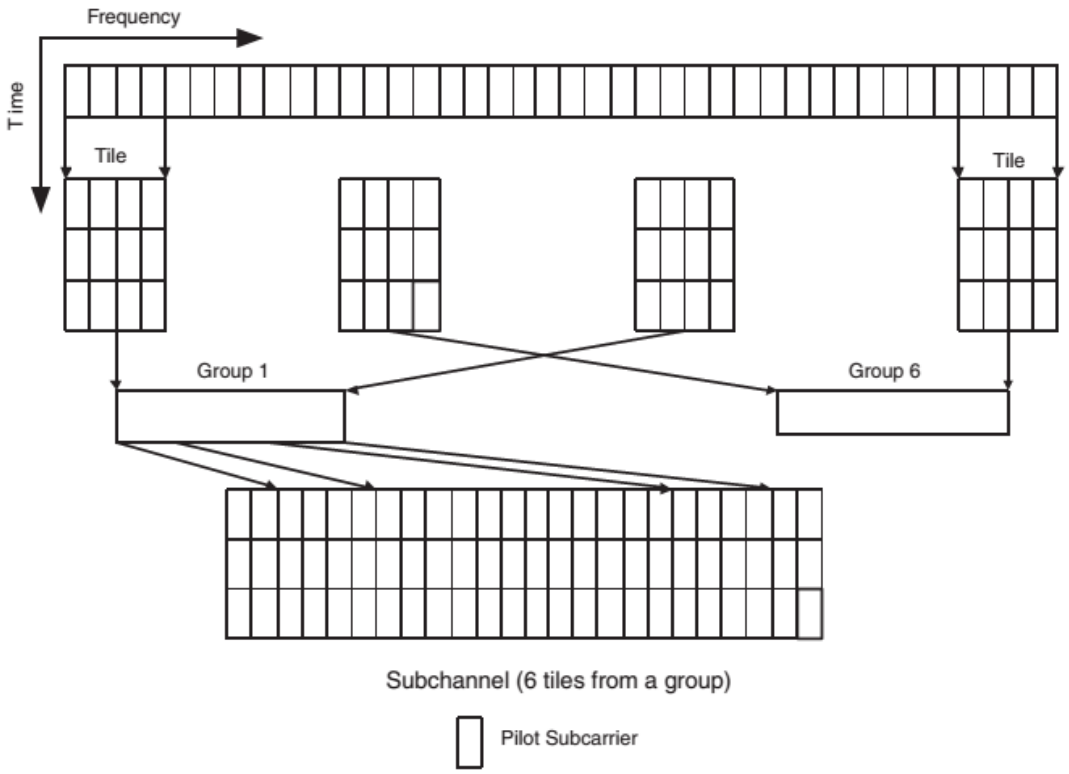

Figure 3.4: UL-PUSC subcarrier permutation scheme [4]

3.2.1 WiMAX DL Subframe

As illustrated in Figure 3.5 DL subframe is made up of multiple sections. The first OFDM symbol is dedicated to preamble which is responsible for synchronization. The preamble is followed by Frame control header (FCH). FCH lasts for one OFDM symbol and contains frame structure information such as coding scheme, MAP message length, available subchannels, and down link frame prefix (DLFP) which indicates the burst profiles and their length for downlink bursts immediately following the FCH. After preamble and FCH there are DL_MAP and UL_MAP. DL-MAP demonstrates the burst profile, location, and duration within the DL frame. The UL-MAP contains control information such as subchannel and slot allocation for the UL subframe. In the frame its position is immediately after the DL-MAP or the DLFP. These are then followed by DCD and UCD which are transmitted by the BS at periodic intervals and express the downlink and uplink frames features respectively.

3.2.2 WiMAX UL Subframe

The UL subframe has quite a different structure as it requires coordination between the various SSs transmitting upwards. It contains contention slots which allow bandwidth requests, initial ranging and one or more uplink PHY PDUs.

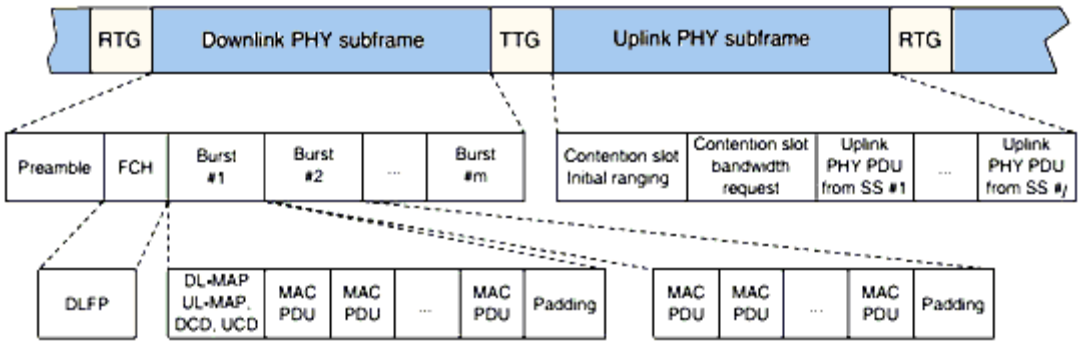

Figure 3.5: WiMAX PHY frame. [8]

Chapter 4

BROADBAND WIRELESS CHANNEL

IEEE 802.16 standards targets to provide a broadband Internet access for mobile users over a wide metropolitan area. Achieving a high data rate for so many users in such a wide area is a challenge. In OFDMA systems, channel estimation is an essential factor for demodulation and coding.

As we know the wavelength of electromagnetic wave is given by $\lambda = \frac{c}{f}$, where f represents the frequency and $c = 3\times10^8$ m/s is the speed of light. Since in UHF bands the wavelength is a fraction of a meter, one would need to determine the location of the receiver and obstacles within some decimeter precision in order to estimate the electromagnetic field accurately.

It's also very important to choose a location to place the base-stations, and what range of power levels are then necessary on the downlink and uplink channels.

4.1 The Broadband Wireless Channel

Generally a communication system consists of two main parts including transmitter and receiver. Transmitted data reach the receiver trough a channel which can alter it. So the information about the way channel alters data should be provided at the receiver. So channel parameters should be estimated. In WiMAX where users are mobile, channel characteristics will also vary in time.

Table 4.1 provides a brief summary of physical parameters of wireless channels.

Table 4.1: Physical parameters of typical fading channel [9]

Parameters	Symbol or Formulas	Representative Values
Distance between BS and MS	d	1 km
User's speed	v	64 km/h
Doppler spread	D_s	100 Hz
Doppler shift	$D = f_c v/c$	50 Hz
Bandwidth	W	1 MHz
Delay spread	T_d	1 μs
Frequency of the carrier	f_c	1 GHz
Time-scale for path amplitude variation	d/v	1 min
Time-scale for path phase variation	$1/(4D)$	5 ms
Coherence time	$T_c = {}^{1}/_{(4D_s)}$	2.5 ms
Coherence bandwidth	$W_c = {}^{1}/_{(2T_d)}$	500 kHz

Equation (4.1) describes the output of a frequency selective channel

$$y[k,t] = \sum_{-\infty}^{\infty} h[j,t]x[k-j] \triangleq h[k,t] * x[k] \tag{4.1}$$

Where, $x[k]$ is an input sequence of data symbols with rate $1/T$ [4] and

$$h[k,t] = h_0\delta[k,t] + h_1\delta[k-1,t] + \cdots + h_v\delta[k-v,t] \tag{4.2}$$

4.2 Multipath Fading Channel

Fading in a wireless channel, is defined as the signal amplitude variation over frequency and time. Small-scale fading and large-scale fading are two main types of Channel fading. Pathloss and shadowing are referred to as Large-scale fading. Multipath fading and time variance are two different types of Small-scale fading. When an electromagnetic wave moves through a large distance, pathloss and shadowing caused by large objects can attenuate it subject to large-scale fading. When a mobile user moves a short distance the constructive and destructive interference of multipath will cause a fast variation of signal level which is referred as small-scale fading. This type of fading depends both on channel characteristic and transmission scheme. A wireless channel can be described by two factors including delay spread and Doppler delay spread. The first one causes time dispersion (frequency-selective fading) and the second one, frequency dispersion (time-selective fading).

4.2.1 Pathloss

Path loss means the reduction in power density of the signal as it passes through the wireless channel. Frii's formula, representing the pathloss for free space is given by:

$$P_r = P_t \frac{\lambda^2 G_t G_r}{(4\pi d)^2} \tag{4.3}$$

Where P_r represents the received power at the receiver, P_t the transmitted power, $\boldsymbol{\lambda}$ the wavelength, G_t the transmitter gain, G_r the receiver gain and d the distance between MS and BS.

Several models are introduced to estimate pathloss in different channels. Okumura, Ericsson, Egli and COST-231[1] Hata model are some examples.

The COST-231 Hata model presented by (4.4) can predict the pathloss in urban, suburban and rural environments for the frequency range from 1500 to 2000 MHz where, h_b is the BS antenna height, d is the distance between MS and BS in kilometers, f is the working frequency in MHz.

$$\text{PL}= 46.3 +33.9 \log_{10} f - 13.82 \log_{10}(h_b) - \text{a}h_m + (44.9-6.55\log_{10}(h_b)) \log_{10} d + c_m \quad (4.4)$$

The value of $c_m$varies for different environments. In suburban environment c_m is equal to zero and in urban environments it is equal to 3. The parameter ah_m which represents the antenna correction factor is given by (4.5) in urban areas and by (4.6) in rural and suburban areas.

$$\text{a}h_m=3.2(\log_{10}(11.75h_r))^2 - 4.79 \quad (4.5)$$

$$\text{a}h_m=(1.11 \log_{10}(f) - 0.7)\, h_r - \log_{10}(f) - 0.8 \quad (4.6)$$

Where h_r is the receiver antenna height in meter.

[1] This empirical channel model is a combination of J.Walfisch and F.Ikegami. It was enhanced by COST 231 project

4.2.2 Shadowing

The attenuation affecting the signal strength caused by obstacles located between transmitter and receiver is referred as shadowing. Since it is impossible to consider all these features in every environment, the shadowing effect is a random process. With the effect of shadowing the general pathloss formula will become as the following formula

$$P_{r=}P_t P_0 \chi \left(\frac{d_0}{d}\right)^a \tag{4.5}$$

Where all the various effects are grouped into two parameters: α which represents the pathloss exponent and P_0 which is the measured pathloss at a reference distance d_0. d_0 can be often chosen as 1 meter and in this case P_0 is well approximated as $(4\pi/\lambda\ )^2$. χ is a sample of shadowing random process, typically modeled as a log normal random variable.

$$\chi = 10^{x/10}\ ,\quad \chi \sim N(0, \sigma_s^2) \tag{4.6}$$

Where, $\chi \sim N(0, \sigma_s^2)$ is a zero mean Gaussian or normal distribution with the variance σ_s^2.

4.3 Cellular system

In cellular systems a vast area is divided into small areas called cells. There is one base station (BS) in each cell and each BS has just the power level to serve users only inside its boundaries, so it is possible to assign the same frequency band to another cell. Adjacent cells are grouped to form a cluster. In each cluster a frequency band is used by only one user.

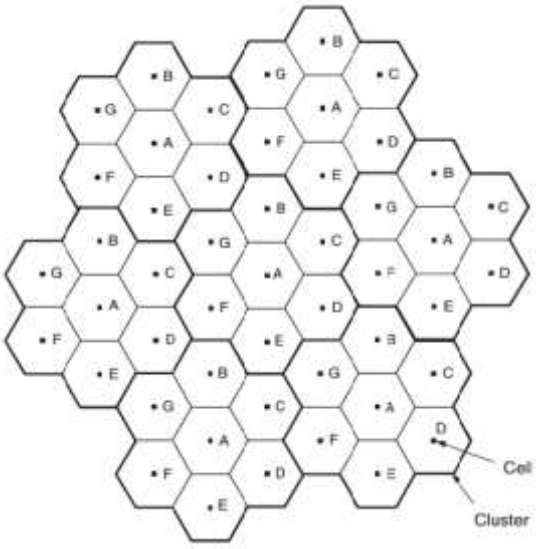

Figure 4.1: A 7-cell cluster replicated over the coverage area for frequency use [9]

Chapter 5

BURST PACKING ALGORITHMS

In mobile WiMAX systems the scheduler manages the resources which should be placed in DL subframe. Due to the restriction of PHY layers each data burst needs to have a rectangular shape. There are several presented packing algorithms trying to minimize the wasted slots in a frame. In this chapter we briefly discuss eOCSA and OBBP algorithms and we introduce MOBBP algorithm which is a modified version of OBBP algorithm.

5.1 Enhanced One Column Stripping with Non-Increasing Area First Mapping (eOCSA) Algorithm

eOCSA which is the improved version of OCSA algorithm tries to pack bursts by minimizing the width of the largest burst and searching for another large burst which can be packed with the same width on top of the previous burst.

The processing starts with sorting of the received bursts in descending order. Secondly, the algorithm calculates smallest possible width for the largest burst, in other word the algorithm divides the area of the largest bust into its maximum possible height and packs it at the bottom right corner of the frame. In the third step the largest burst which can be packed on top of the previous burst will be selected. The widths of the bursts in this step are pre-determined. The process will be repeated until there is no appropriate burst or there is no space on top the first column. The

algorithm moves leftward and the second and third steps will be repeated for the remaining columns.

5.2 Orientation-Based Burst Packing (OBBP) Algorithm

OBBP algorithm is a burst packing algorithm which lets the bursts have just rectangular shapes and each rectangle can have more than one dimension. This dimension is selected in such a way to use the frame in an optimal manner. In this algorithm the bursts are grouped up considering different orientation factors they have and then each group is packed in column-wise or row-wise in the down-link subframe. Orientation factors of a burst means the set which contains all the orientations that the rectangular shape burst can have. In other word the set containing any combinations of the burst size. For example considering a burst of size 20 the set of orientation factors is $\{1 \times 20, 2 \times 10, 4 \times 5, 5 \times 4, 10 \times 2, 20 \times 1\}$. Choosing one of these possible OFs to put the burst in the frame is one of the most challenging parts of OBBP algorithm. OBBP algorithm is generally divided into three main stages. In first stage named pre-packing stage all possible OFs for each burst are calculated. Then useless ones are removed. Useless means OFs which are out of Frame range. Finally we arrange the bursts sizes in a matrix (OF_Matrix) based on these OFs. In second stage which is the main stage using OF_Matrix packing sets are selected considering their common OFs. Finally the third stage tries to pack as many of the remaining bursts from stage II. To utilize free slots remaining in the DL-subframe the conventional best-fit algorithm is used.

5.3 Modified Orientation-Based Burst Packing (MOBBP) Algorithm

MOBBP algorithm which is a modified version of OBBP improves the packing efficiency by making some modifications in third stage of OBBP. There are also some amendments in the way of burst adaptation and allocation of bursts with the same size.

5.3.1 Pre-packing Stage

Since the total size of the received set of bursts that the scheduler has assigned can be greater than the capacity of the DL-subframe a set of operations need to be performed before the main packing stage. Below are some of these operations that the pre-packing stage has to perform.

5.3.1.1 Priority Sorting

A set of *n* sorted bursts (*B*) is sent to our algorithm. Sorting the bursts is already done by scheduler considering QoS provisioning. As the total number of slots in *B* may be more than the frame size we choose the first *m* bursts which can be fitted in the frame and we call it B'.

$$B=\{b_1, b_2, \dots, b_m, \dots, b_n\}$$
$$b_1 + b_2 + b_3 + \cdots + b_n > N \quad slots \tag{5.1}$$

$$B'=\{b_1, b_2, \dots, b_m\}$$
$$b_1 + b_2 + b_3 + \cdots + b_n \leq N \quad slots \tag{5.2}$$

The set of remaining bursts *B*- B' will be considered in the next frame.

5.3.1.2 OF Calculation

To calculate OF for each burst first of all we should find the set of all divisors for the integer representing the burst size.

As we know the residue of dividing an integer to its divisor is zero.

$$\text{Divisors} = \{j = 1,2,\dots, b_i \mid \forall\, i \leq m\,, mod(b_i\,, j) = 0\ \} \tag{5.3}$$

This way we find the set of positive divisors for each member of B'. Putting together the first and the last divisors we generate an OF. The second OF is the combination of the second and the penultimate divisor, and so on.

5.3.1.3 Constructing OF Matrix

OF_Matrix is a matrix in which burst sizes are putted in rows and columns determined by their OFs. Other elements are zero.

Firstly we generate a Zero matrix and then according to OFs we enter members of B' in the Matrix.

Consider we have B' as follows.

$$B' = \{10,7,4,6,10,9,4,10\} \tag{5.4}$$

OFs for this set of bursts will be$\{1 \times 7\,, 7 \times 1\}$,$\{1 \times 4\,, 2 \times 2\,, 4 \times 1\}$,$\{1 \times 6\,, 2 \times 3, 3 \times 2\,, 6 \times 1\}$, $\{1 \times 10\,, 2 \times 5\,, 5 \times 2, 10 \times 1\}$, $\{1 \times 9\,, 9 \times 1\}$.

As the maximum number is 10 we generate a 10×10 zero matrix in which we enter the burst sizes. Matrix (5.5) shows the OF_Matrix for B'.

$$\text{OF\_Matrix}=\begin{bmatrix} 0 & 0 & 0 & 4 & 0 & 6 & 7 & 0 & 9 & 10 \\ 0 & 4 & 6 & 0 & 10 & 0 & 0 & 0 & 0 & 0 \\ 0 & 6 & 0 & 0 & 0 & 0 & 0 & 0 & 0 & 0 \\ 4 & 0 & 0 & 0 & 0 & 0 & 0 & 0 & 0 & 0 \\ 0 & 10 & 0 & 0 & 0 & 0 & 0 & 0 & 0 & 0 \\ 6 & 0 & 0 & 0 & 0 & 0 & 0 & 0 & 0 & 0 \\ 7 & 0 & 0 & 0 & 0 & 0 & 0 & 0 & 0 & 0 \\ 0 & 0 & 0 & 0 & 0 & 0 & 0 & 0 & 0 & 0 \\ 9 & 0 & 0 & 0 & 0 & 0 & 0 & 0 & 0 & 0 \\ 10 & 0 & 0 & 0 & 0 & 0 & 0 & 0 & 0 & 0 \end{bmatrix} \quad (5.5)$$

The OF_Matrix in this step is symmetric as it is a square matrix symmetric about its main diagonal.

5.3.1.4 Burst Adaptation

Burst adaptation means removing bursts with OFs out of the frame range from the OF_Matrix. Assume that we have a 60×14 DL subframe and a burst of size 80. This burst cannot be packed in the frame by OFs 1×80 or 80×1.

To remove these OFs from the OF_Matrix we cut the matrix from its 61^{th} row and 15^{th} column.

Cutting the OF_Matrix we may lose some bursts. That means burst which have no OFs within the frame range. The algorithm suggests them to be incremented. For example a burst of size 67, with OFs $\{1 \times 67 , 67 \times 1\}$ cannot be packed in the frame. Incrementing it, we can pack 68 with multiple OFs in the frame range. It is possible that an incremented burst still remains without any OF in the frame range; we will increment it once more. For example consider a 30×12 subframe and a burst of size 73. After the first increment we have 74 ($\{1 \times 74 , 2\times 37 , 37\times 2 , 74\times 1 \}$) which doesn't have any appropriate OF again. This time the algorithm

tries to pack 75 with the following OFs in the frame range $\{3 \times 25,\ 5 \times 15, 15 \times 5, 25 \times 3\}$.

Doing burst adaptation OF_Matrix will not be a square matrix anymore.

5.3.1.5 Construction of Repetition Matrix

As the algorithm chooses the subsets of bursts using an OF_Matrix and then sets their position to zero, standard OBBP does not support each burst size more than once. To prevent losing the same size bursts we have introduced RP_Matrix which contains number of repetition for each burst.

For example for B' represented in (5.4) burst sizes 4 and 10 are repeated respectively twice and tree times so RP_Matrix will be constructed as follows:

$$\text{Rp\_Matrix}=\begin{bmatrix} 0 & 0 & 0 & 2 & 0 & 1 & 1 & 0 & 1 & 3 \\ 0 & 2 & 1 & 0 & 3 & 0 & 0 & 0 & 0 & 0 \\ 0 & 1 & 0 & 0 & 0 & 0 & 0 & 0 & 0 & 0 \\ 2 & 0 & 0 & 0 & 0 & 0 & 0 & 0 & 0 & 0 \\ 0 & 3 & 0 & 0 & 0 & 0 & 0 & 0 & 0 & 0 \\ 1 & 0 & 0 & 0 & 0 & 0 & 0 & 0 & 0 & 0 \\ 1 & 0 & 0 & 0 & 0 & 0 & 0 & 0 & 0 & 0 \\ 0 & 0 & 0 & 0 & 0 & 0 & 0 & 0 & 0 & 0 \\ 1 & 0 & 0 & 0 & 0 & 0 & 0 & 0 & 0 & 0 \\ 3 & 0 & 0 & 0 & 0 & 0 & 0 & 0 & 0 & 0 \end{bmatrix} \tag{5.6}$$

This matrix will be used in main packing stage and if a burst size is repeated more than once it will prevent setting its position to zero before allocating all of them. Number of repetitions in this matrix will be subtracted by one after each selection.

5.3.2 Main Packing Stage

The main idea of OBBP algorithm is to reduce the complexity of finding optimal location for rectangular bursts. Optimal location means minimizing the irregularity

of unallocated slots after each burst packing. To achieve this as illustrated in Figure 5.1 we start from bottom-right corner of the frame and try to fill up all rows (vertically) or all columns (horizontally) with bursts in the same column of OF_Matrix (bursts which will occupy the same number of symbols).

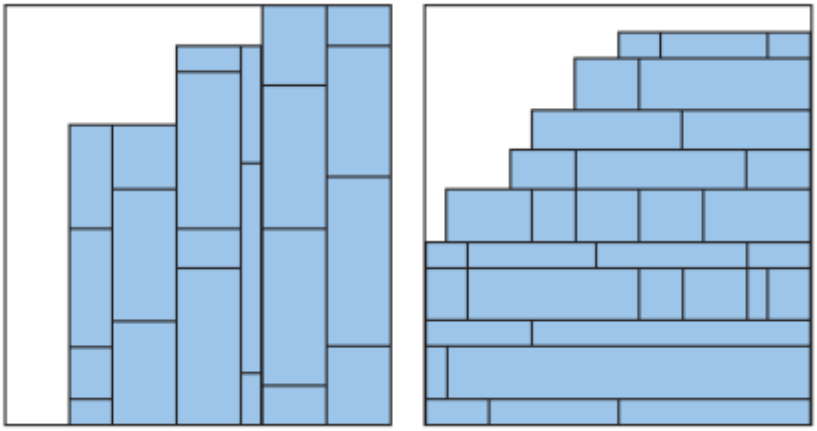

Figure 5.1: Vertical and horizontal allocation in OBBP algorithm [11]

This algorithm will result a staircase like shape which will facilitate using unallocated slots to pack more bursts. Now steps leading us to generate the staircase like shape will be explained.

5.3.2.1 Packing Set Selection

OF_Matrix helps us to find out which bursts can have the same number of symbols (vertical allocation) or subchannels (horizontal allocation). For example referring to OF_Matrix in (5.5) we can allocate {4, 6, 10} together with the same number of symbols which is 2 or the same number of subchannels which is also 2. In this thesis we will do all allocations vertically.

Usually the QoS provisioned by OFDMA systems gives the highest priority to burst with larger sizes. The column containing maximum number of bursts may contain many of small bursts or few of larges or a combination of both. In this

algorithm we try to fill up each column as much as possible and large size bursts are prior.

A stairs-like shape should be achieved in our frame so we start packing with maximum number of slots. Four steps followed to select packing sets are as following.

a. Finding the column which has the maximum sum of elements. For example consider a 60×14 OF_Matrix constructed based on the following set of bursts sizes.

   $B' = \{4, 18, 14, 24, 17, 14, 50, 73, 76, 21, 41, 32, 44, 24, 9, 37, 17, 6, 77, 37, 78\}$

   Sum of elements in each column will be

   317 420 156 180 50 126 112 56 27 50 121 24

   So the second column is selected in this step. We call this set B'_{max}.

   B'_{max} = {4, 6, 14, 18, 24, 32, 44, 50, 74, 76, 78}

b. Arranging B'_{max} in descending order. This arrangement is done to give more priority to larger bursts.

   B'_{max}= {78, 76, 74, 50, 44, 32, 24, 18, 14, 6, 4}

c. Finding the rectangles length of B'_{max}. In This example the selected column was the second one so all rectangles have the width 2. The set of rectangle lengths ($B'_{\max\_L}$) will be burst sizes divided by their width.

   $B'_{\max\_L} = \{39, 38, 37, 25, 22, 16, 12, 7, 3, 2\}$

d. Finding the optimal subset of bursts. Sum of the length of these selected rectangles is more than 60 (Number of subchannels) $\sum B'_{\max\_L}$= 201 >60 so we cannot allocate all them together. Now bursts with closest sum to 60 are chosen. As large size bursts have more priority we try to use them first. In

this example {38, 22}, {37, 16, 7}, {39, 12, 7, 2} can all fill the frame up to 60^{th} subchannel. The first subset contains less number of bursts but larger size ones so this subset is chosen.

After selection of optimum subset all elements in OF_Matrix with that amount will be set to zero. Here RP_Matrix is used to prevent setting the repeated burst sizes to zero. For example if for a burst size the corresponding element in RP_Matrix is 3 which means that burst size is repeated tree times in B',after the first selection of this burst 3 will be changed to 2 in Rp_Matrix. Elements in OF_Matrix will be set to zero only if the corresponding element in Rp_Matrix is 1. We will repeat these steps from ‘a.’ to ‘d.’ until all elements in OF_Matrix will become zero.

5.3.2.2 Packing Set Arrangement

Now all bursts are posed in a group to allocate. In this step we calculate sum of each group and rearrange them in descending order. As closer the sum is to 60 the subset of bursts will enter the subframe sooner. This way the algorithm forms a stairs-like shape.

5.3.2.3 Packing Set Stuffing

We start packing bursts from the bottom-right corner of the subframe. According to the width of each group of bursts (number of symbols) we pack all subsets next together until no more subsets can enter the subframe which means there are no more columns in the subframe. In this step unallocated slots will remain at the top-left and they will be used in next step to allocate remaining bursts.

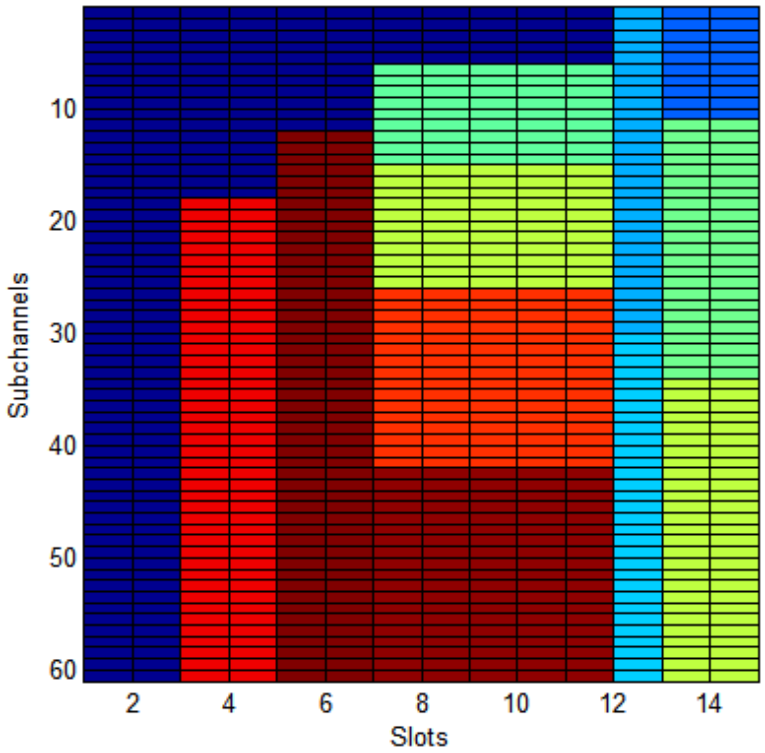

Figure 5.2: Stairs-like shape produced by allocated slots

5.3.3 Packing Remaining Bursts

In this step we try to use the unallocated slots to pack remaining bursts. As we succeeded to minimize the deformation of free space, the remaining bursts have more opportunity to be packed in the subframe. In this section proposed steps to pack remaining bursts are discussed.

a. Sorting remaining bursts in descending order. As larger bursts have more priority than small ones and also as they are less probable to find a suitable position we start with packing larger one.
b. Dividing unallocated slots into rectangles with its maximum possible dimension. As some bursts may require more space besides dividing the free space horizontally and vertically, we consider also larger rectangles as illustrated in Figure (5.3 (c)).

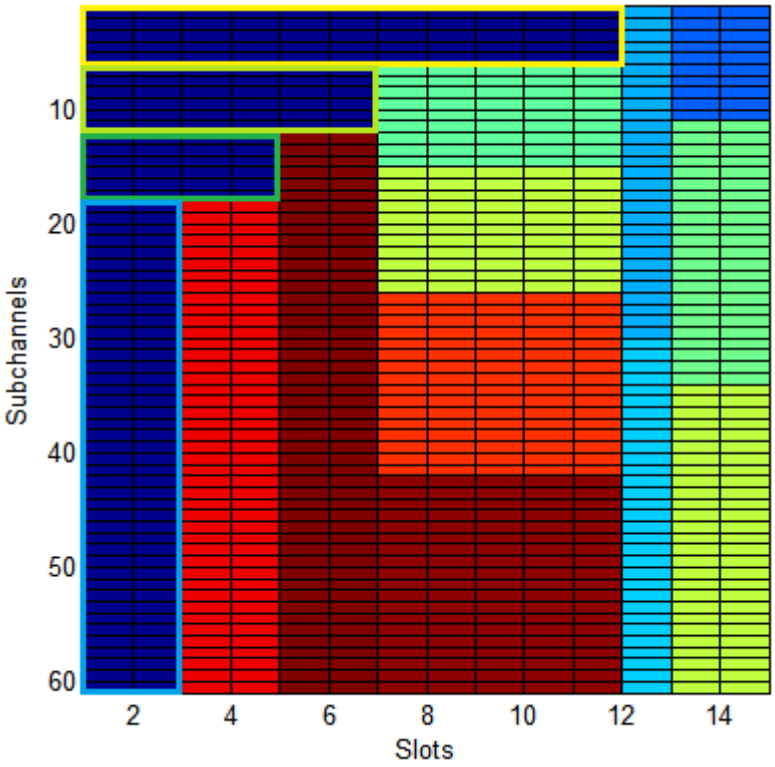
Subchannels
10
20
30
40
50
60
2
4
6
8
10
12
14
Slots

(a)

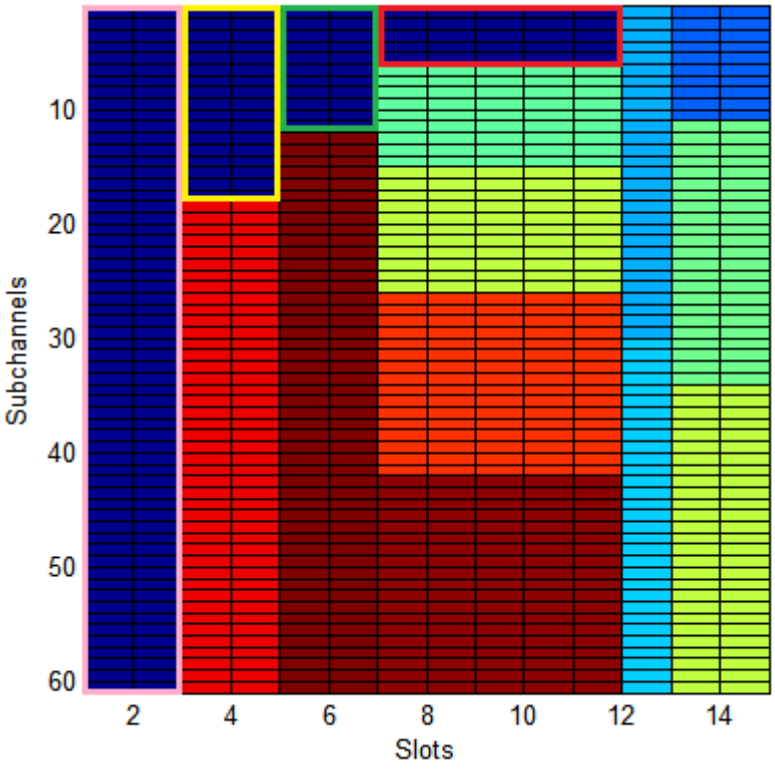
Subchannels
10
20
30
40
50
60
2
4
6
8
10
12
14
Slots

(b)

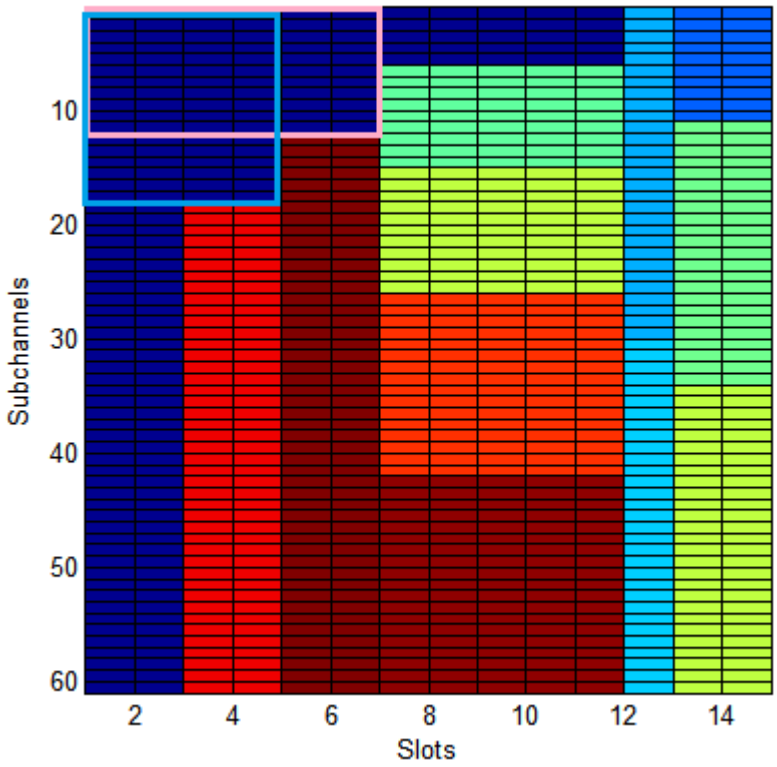

(c)

Figure 5.3: Dividing Free Slots into Rectangles
a) Horizontal Rectangles
b) Vertical Rectangles
c) Large Rectangles

c. Choosing the suitable rectangle for the burst. Based on OF_Matrix for remaining bursts, we decide if a burst can be fitted in each rectangle or no. If there is more than one rectangle for a burst, we will choose the rectangle with the minimum difference with the burst size. If there is no rectangle which can fit the burst with its orientation the OBBP algorithm will drop it and repeats the procedure for other bursts if any. In MOBBP we increment such bursts and retry to pack it in the frame. For example consider a burst of size 33 and remaining rectangles with sizes $\{4 \times 5, 3 \times 3,\ 2 \times 20,\ 2 \times 27,\ 3 \times 7\}$. Orientation Factors for 33 are $\{1 \times 33,\ 3 \times 11,\ 11 \times 3,\ 33 \times 1\}$. So 33 cannot enter any rectangle. Incrementing 33, we can easily pack 34 (2×17) in forth rectangle.

d. Fitting the burst in the selected rectangle. After finding the suitable rectangle we pack the burst in its bottom-right corner.

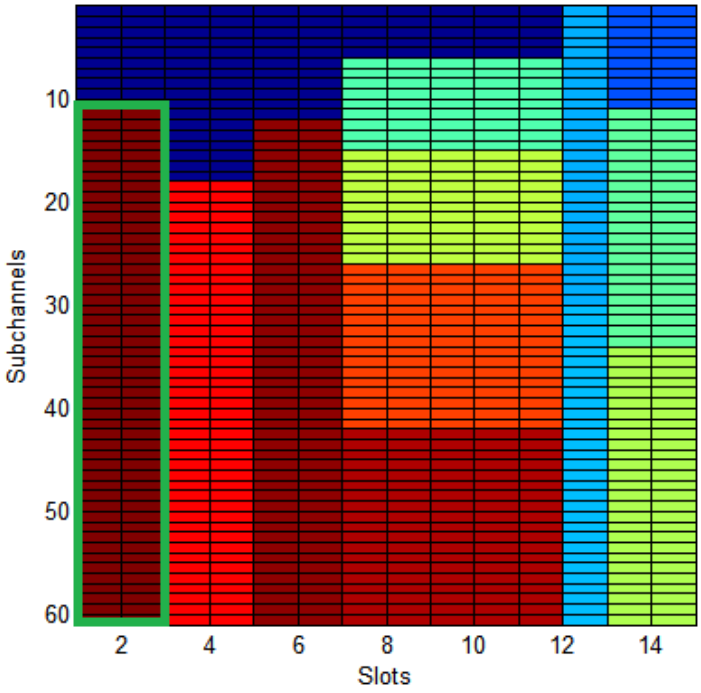

Figure 5.4: Fitting the remaining bursts in the frame

When the first remaining burst is allocated, we re-measure the remaining free space and repeat the steps form ‘a’ to ‘d’ for the rest of burst. Figure 5.5 depicts the DL subframe after stage III packing.

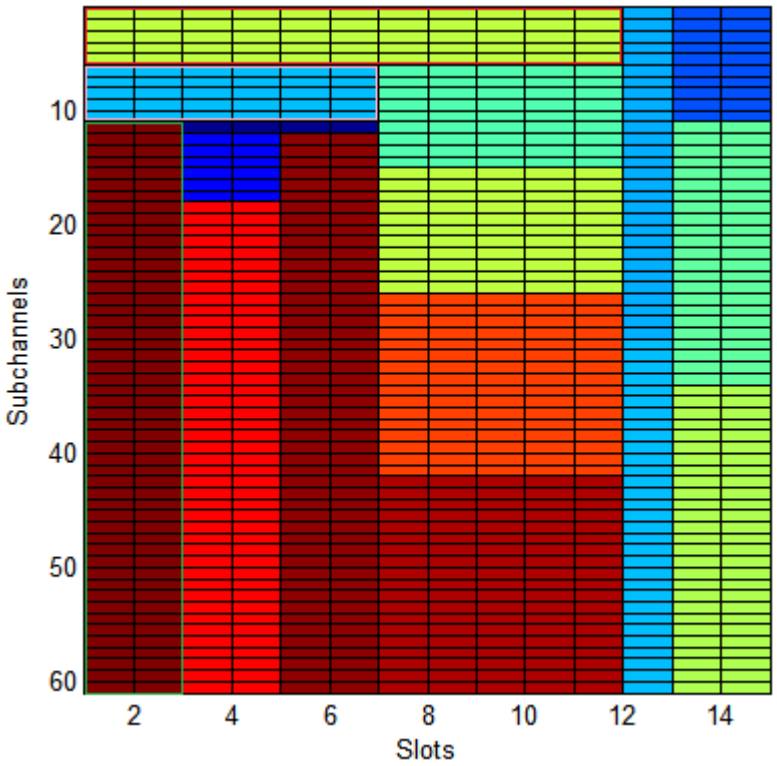

Figure 5.5: Fitting the Remaining bursts in the frame

Chapter 6

PERFORMANCE EVALUATION OF PROPOSED PACKING ALGORITHM

In this chapter, simulation results are presented and the performance of MOBBP algorithm is evaluated and compared with OBBP algorithm in terms of Packing efficiency, number of padded slots and number of dropped bursts.

Constructing an OF_Matrix each burst size is placed in the matrix in such a way that the number of column multiplied by the number of row will give the value of each element and all other elements are zero. When a burst enters the DL subframe all elements in OF_Matrix with the same value are set to zero so if a burst size is repeated more than once OBBP algorithm will remove the repeated ones. Introducing RP_Matrix which contains number of repetition for each burst size we prevent losing them.

Besides, in third stage of OBBP algorithm when a burst does not find a suitable rectangle based on its OFs it will be dropped while MOBBP algorithm increments it and retries to pack it. Figure 6.1 (a) illustrates a 60×14 DL subframe packed by OBBP algorithm where [77 63 21] are remaining bursts at the end of stage 2. 77 cannot be packed in any of the overlapped rectangles. OBBP drops it and packs 63 and 21. Figure 6.1 (b) illustrates the same bursts packed by MOBBP algorithm where 78 and 64 are packed instead of 77 and 63 respectively and 21 will be dropped.

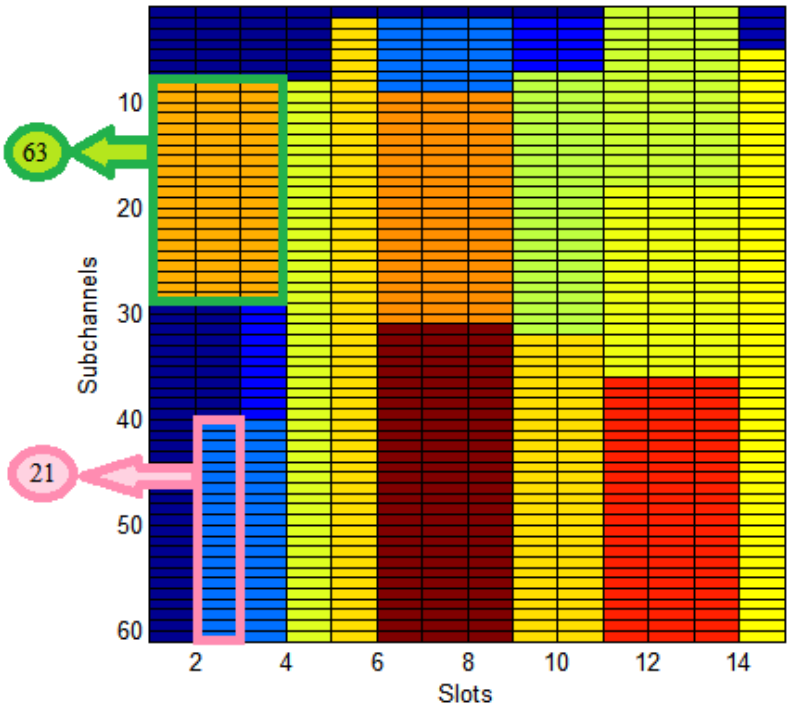

(a)

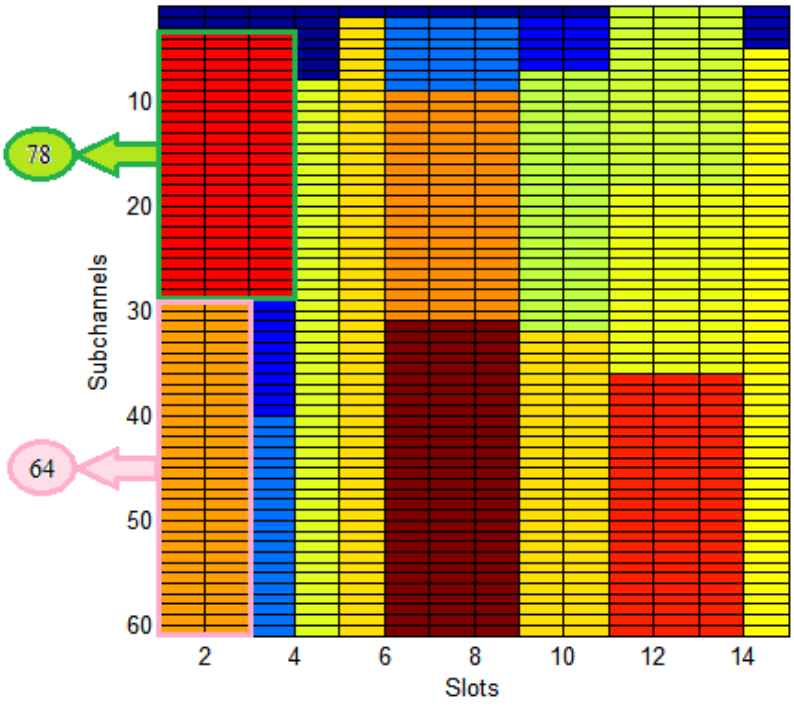

(b)

Figure 6.1: Frame Packed by a) OBBP b) MOBBP Algorithm

6.1 Frame Packing For Randomly Generated Burst Sizes

In this section simulation results for randomly generated bursts are provided. The performance of the proposed algorithm is evaluated for a 14 × 60 DL subframe with frame duration of 5 ms and 10 MHz subchannel. The Packing efficiency of the algorithm is calculated using (6.1) for 1000 frames under different loads.

$$\eta_{pk} = \frac{S_{total} - S_{padded}}{S_{total}} \ \% \tag{6.1}$$

In this case $\eta_{pk} = \frac{(Nsch \times Nslots) - S_{padded}}{(Nsch \times Nslots)}$ where S_{padded} comprises number of over allocated slots. Burst size ratio given by (6.2) is set to 50%.

$$BSR = \frac{B_{small}}{B_{large}} \tag{6.2}$$

B_{th} is the burst size threshold which is set to 20. Bursts larger than 20 are considered as large size and smaller ones are small bursts. Burst sizes are randomly generated in the range [2, 95].

6.1.1 Packing Efficiency

Figure 6.2 demonstrates the Packing efficiency of OBBP and MOBBP algorithms under different loads. The packing gain varies from 1.3 percent and it is more distinct around the frame capacity (instantaneous load of 1).

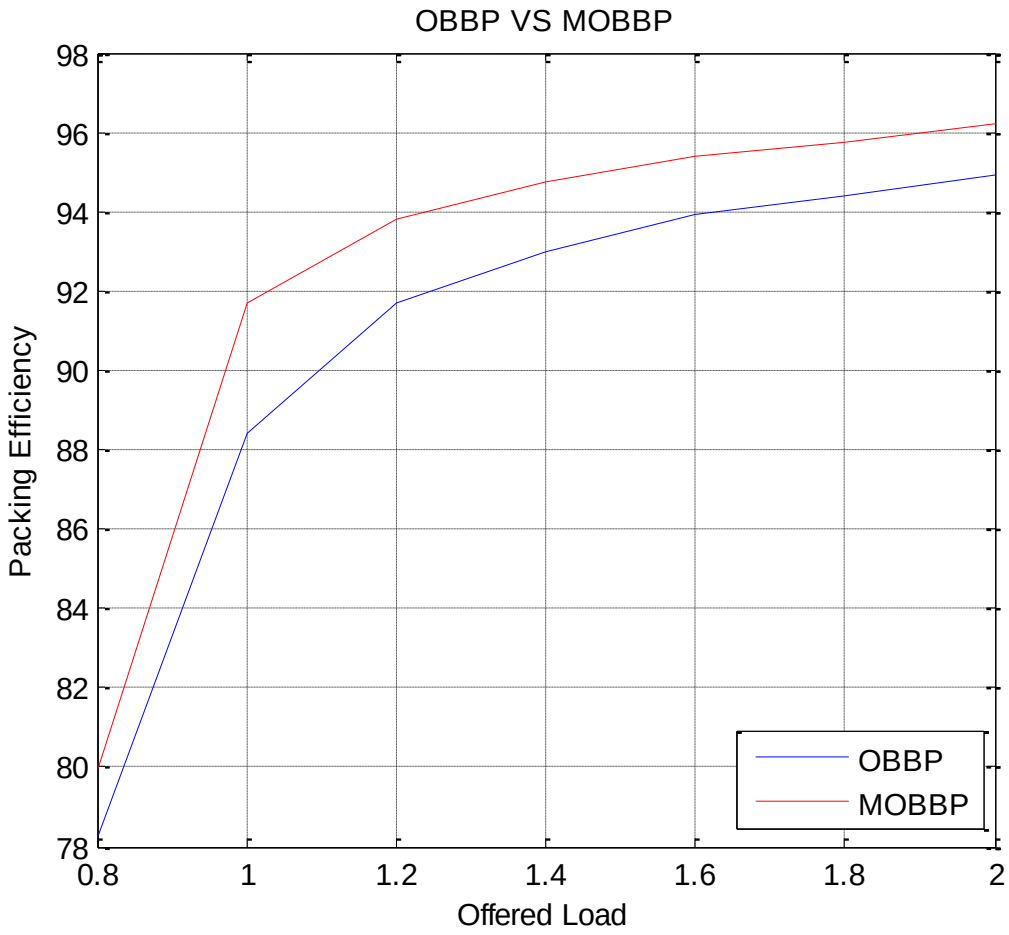

Figure 6.2: Packing Efficiency of OBBP and MOBBP Algorithms

In Figure 6.3 the Packing efficiency of the two algorithms are also compared with eOCSA

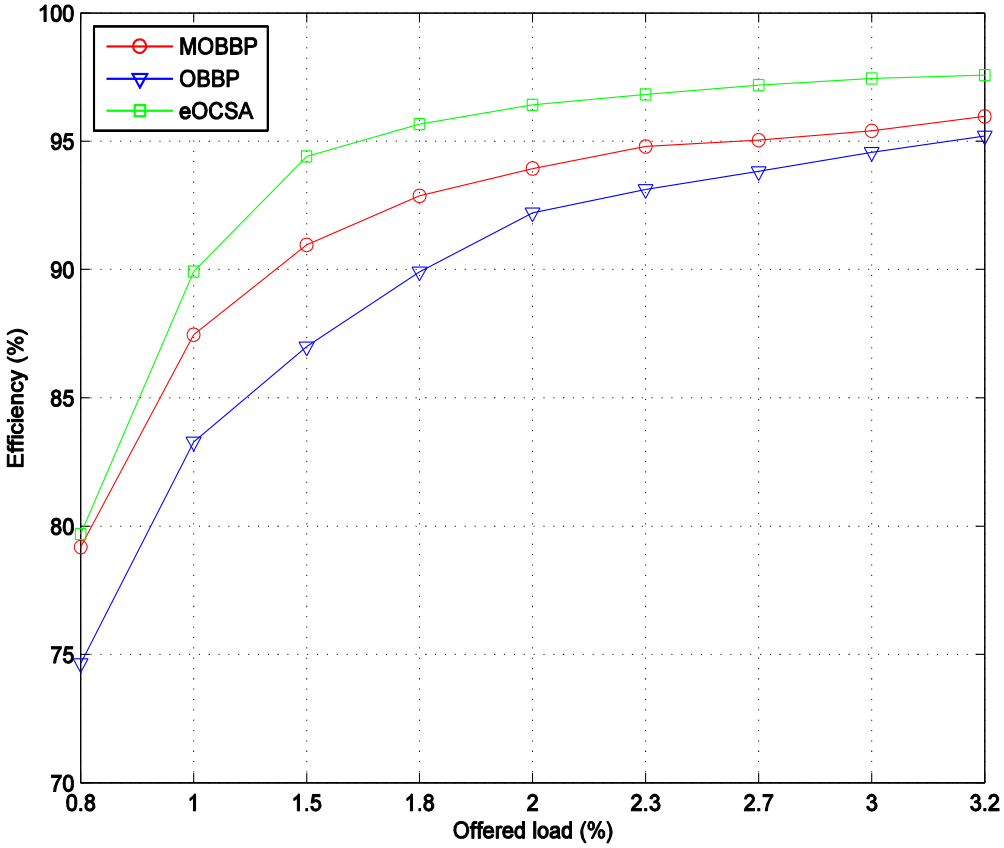

Figure 6.3: Packing efficiency of OBBP, MOBBP and eOCSA

6.1.2 Over Allocations

As in MOBBP we try to pack more bursts by over allocation, number of padded slots is more than MOBBP. Figure 6.4 depicts number of padded slots in OBBP and MOBBP algorithms.

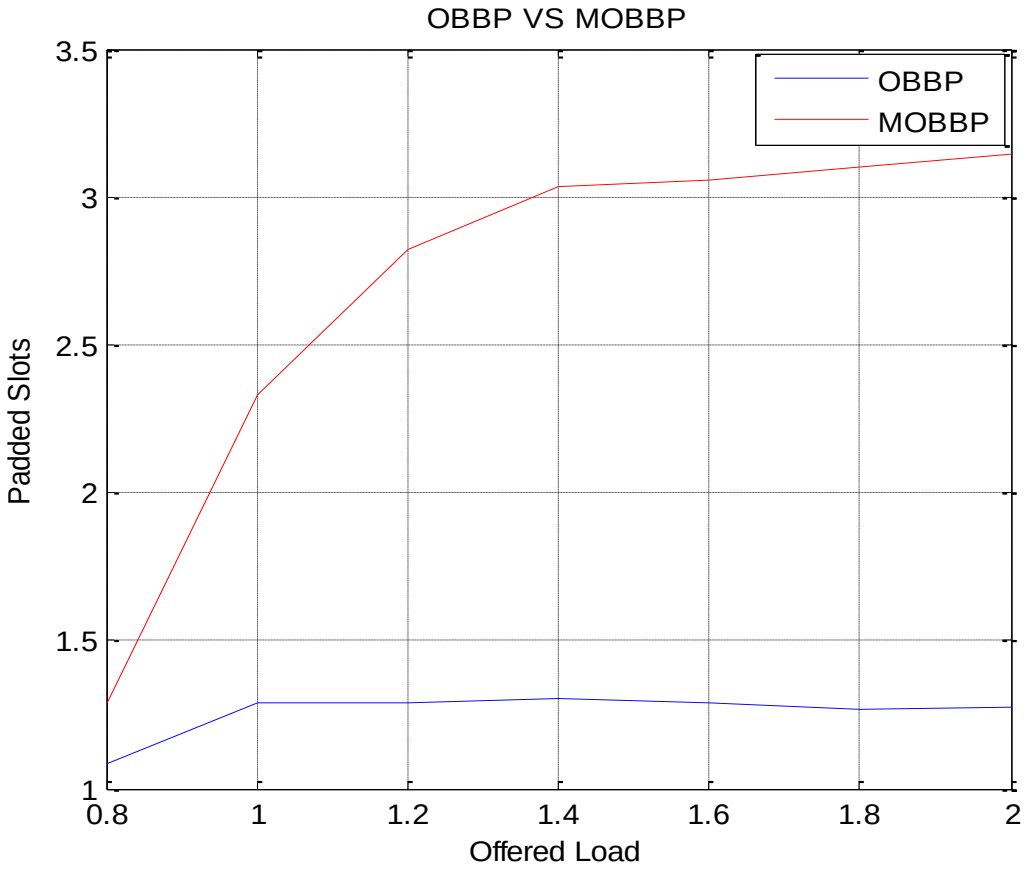

Figure 6.4: Number of Padded Slots in OBBP and MOBBP Algorithms

6.1.3 Number of Drops

Figure 6.5 compares number of dropped bursts in OBBP and MOBBP algorithms. MOBBP algorithm in the third stage over allocates bursts which can find a rectangle with the required area but not appropriate OF, so it prevents the burst to be dropped on the other hand it may drop a smaller burst as the frame capacity gets full. So the difference in numbers of drops between the two algorithms is not so distinct. As the graph illustrates number of dropped bursts has been totally reduced in MOBBP particularly around the frame capacity.

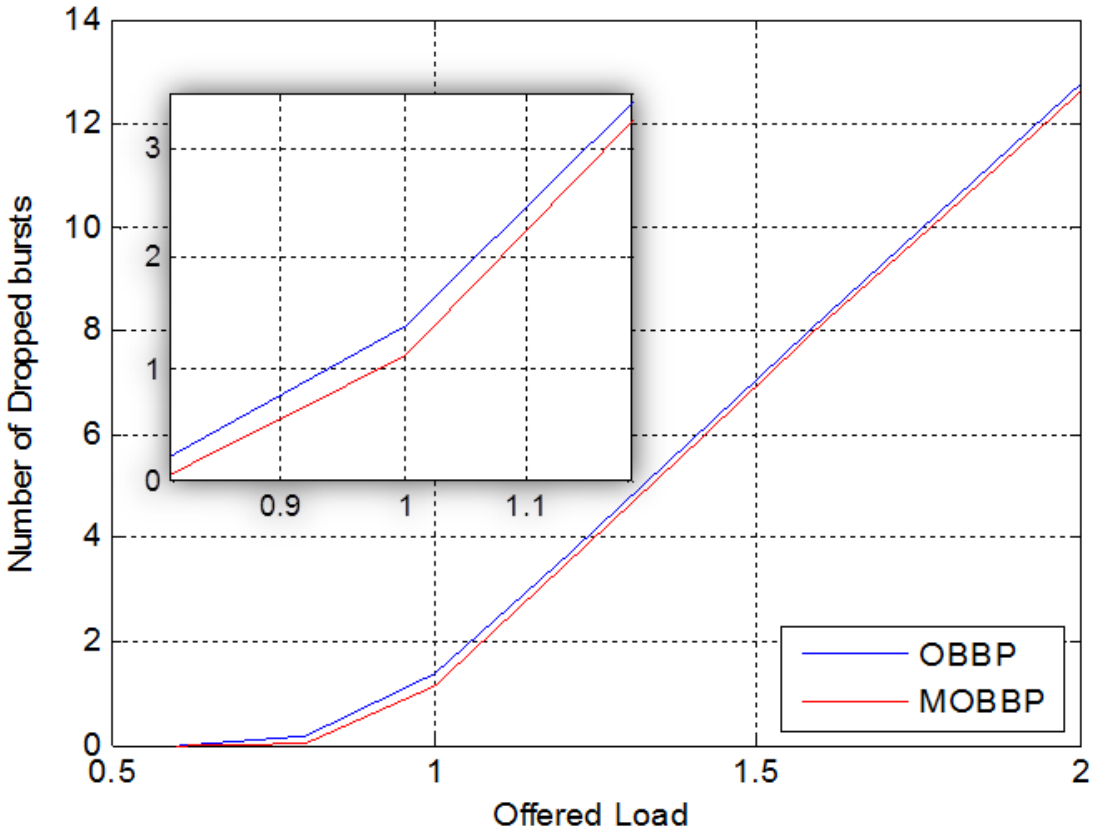

Figure 6.5: Number of Dropped Bursts in OBBP and MOBBP Algorithms

6.2 Frame Packing Using the COST-231 Extended Hata Channel Model

In this section we present the simulation results for the algorithms under real traffic where the COST-231 Hata model is selected as the channel model. User's distance from base station and user's speed have been uniformly distributed .Number of Users change from 20 to 40. Packing efficiency and number of padded slots in the two algorithms are compared for different number of users.

6.2.1 Packing Efficiency

Figure 6.6 depicts the packing Efficiency of OBBP and MOBBP algorithms in the real channel model. And Figure 6.7 compares the Packing Efficiency of OBBP, MOBBP and eOCSA in the same channel.

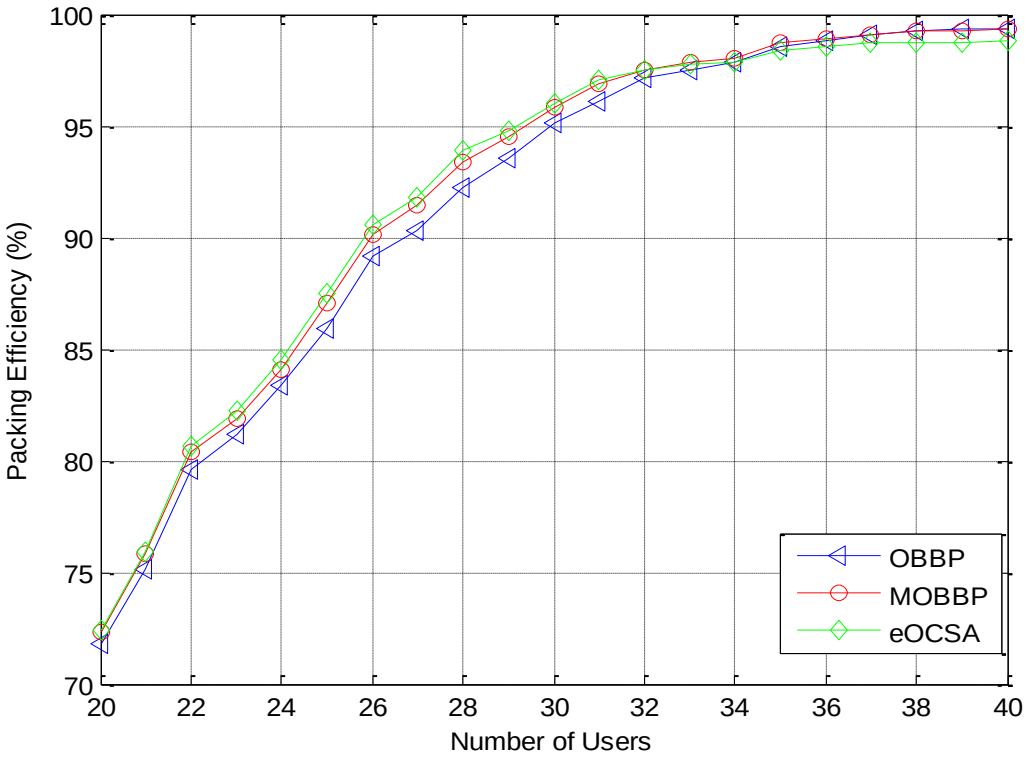

Figure 6.6: Packing Efficiency of OBBP, MOBBP and eOCSA Algorithms

Chapter 7

CONCLUSION AND FUTURE WORKS

7.1 Conclusion

In this thesis we have worked on OBBP as an effective burst packing algorithm which groups up the bursts based on their orientation factors. We have introduced a new packing strategy in the third stage of the well-known OBBP frame packing algorithm that helps attain better utilization of the available free space in the DL subframe and hence leads to an increased frame packing efficiency.

The OBBP, MOBBP and eOCSA algorithms were compared for randomly generated bursts and for bursts sizes obtained while using the COST-231 Extended Hata channel model. It was observed that efficiency of MOBBP algorithm is 1-3 percent better than OBBP for randomly generated bursts and about 3-9 percent for the realistic channel model. Also the efficiency of eOCSA is better than OBBP and MOBBP for randomly generated bursts. Mean over allocations per frame for eOCSA is much higher than that of MOBBP and OBBP.

7.2 Future Work

Simulation results have shown that the packing efficiency of the MOBBP was improved for all instantaneous offered loads. The gain in packing efficiency could easily be justified considering the small increase in over allocations that the new strategy of MOBBP algorithm has brought. In the future in order to provide services with desired levels of QoS we can work on a priority-aware version of MOBBP algorithm which can give priority to allocation of bursts based on latency constraints. Also, since in real life the allocator is fed by a scheduler in the MAC layer, future work will involve the study and simulation of throughput maximizing and QoS aware frame based or time-stamp based schedulers.

REFERENCES

[1] L. Nuaymi, *WiMAX Technology for Broadband Wireless Access,* ENST Bretagne: John Wiley & Sons Ltd, 2007.

[2] IEEE 802.16-2004, *IEEE Standard for Local and metropolitan area networks Part 16: Air Interface for Fixed Broadband Wireless Access Systems*, New York, 1 October 2004.

[3] "*Mobile WiMAX – Part I:A Technical Overview and Performance Evaluation*," WiMAX Forum, August, 2006.

[4] J. G. Andrews, A. Ghosh, R. Muhamed, F*undamentals of WiMAX Understanding Broadband Wireless Networking*, Westford, Massachusetts.: Prentice Hall, February 2007.

[5] H. Schulze and C. Lueders, *Theory and Applications of OFDM and CDMA Wideband Wireless Communications*, Meschede, Germany: John Wiley & Sons Ltd., 2005.

[6] Y. S. Cho, J. Kim, W. Y. Yang, C. G. Kang, *MIMO-OFDM Wireless Communications With MATLAB*, Clementi Loop, Singapore: John Wiley & Sons (Asia) Pte Ltd, 2010.

[7] R. Prasad, *OFDM for Wireless Communications Systems*, Boston ,London: Artech House, Inc., 2004.

[8] IEEE 802.16e, *IEEE Standard for Air Interface for Broadband Wireless Access Systems_Amendment 2: Higher Reliability Networks*, Piscataway, 6 March 2013.

[9] D. Tse , P. Viswanath, *Fundamentals of Wireless Communication*, Cambridge university press, 2005.

[10] M. Alshami, T. Arslan, J. Thompson and A. Erdogan, "*Evaluation of Path Loss Models at WiMAX Cell- edge*," Edinburgh,Scotland, UK, 2011.

[11] O. M. Eshanta, M. Ismail, and K. Jumari, "OBBP: An Efficient Burst Packing Algorithm for IEEE 802.16e Systems," *International Scholarly Research Network ISRN Communications and Networking*, Vol. 2011, Article ID 734297,, no. 10, pp. 1-9, 2011.

[12] C. So-In, R. Jain, A-K. A. Tamimi, "OCSA: An Algorithm for Burst Mapping in IEEE 802.16e Mobile WiMAX Networks1,2," in *Proceedings of the 15th Asia-Pacific Conference on Communications (APCC 2009)-013*, Oct., 2009.

[13] C. So-In, R. Jain, and A-K. A. Tamimi, "eOCSA: An Algorithm for Burst Mapping with Strict QoS Requirements in IEEE 802.16e Mobile WiMAX

Networks," 2009.

[14] T-H. Lee, C-H. Liu, J. Yau and Y-W. Kuo, "Maximum Rectangle-Based Down-Link Burst Allocation Algorithm for WiMAX Systems," in *TENCON 2011* , Bali, 2011.

[15] K. Bahmani, E. A. Ince, D. Arifler, "Priority-Aware Downlink Frame Packing Algorithm for OFDMA-Based Mobile Wireless Systems," in *Signal Processing and Communications Applications Conference (SIU)*, 2013.

[16] D. Alam and R. H. Khan, "Comparative Study of Path Loss Models of WiMAX at 2.5 GHz Frequency Band," *International Journal of Future Generation Communication and Networking*, Vols. 6, No. 2, p. 14, April, 2013.

[17] J. Vanderpypen and L. Schumacher, "Treemap-based Burst Mapping Algorithm for Downlink Mobile WiMAX Systems," in *Vehicular Technology Conference*, 2011.

[18] R. Mardeni, T. S. Priya, "Optimised COST-231 Hata Models for WiMAX Path Loss Prediction in Suburban and Open Urban Environments," *Modern Applied Science*, Vols. 4, No. 9, p. 15, September 2010.

[19] D. Pareit, B. Lannoo, I. Moerman and P. Demeester, "The History of WiMAX: A Complete Survey of the Evolution in Certification and Standardization for IEEE 802.16 and WiMAX," *IEEE Communications Survey & Tutorials*, Vols.

14, No.4, p. 29, Fourth quarter 2012.